Universidade do Minho
Escola de Engenharia

Ana Patrícia Ribeiro Gonçalves

Set-up and optimization of a pilot-scale photobioreactor for autotrophic microalgae growth

December 2021

Set-up and optimization of a pilot-scale photobioreactor for autotrophic microalgae growth
Ana Patrícia Ribeiro Gonçalves
UMinho 2021

Universidade do Minho
Escola de Engenharia

Ana Patrícia Ribeiro Gonçalves

Set-up and optimization of a pilot-scale photobioreactor for autotrophic microalgae growth

Master's Thesis

Integrated Master in Biological Engineering

Environmental Technology

Work developed under the guidance of:

Professor José António Teixeira

December 2021

DECLARAÇÃO DE AUTOR E CONDIÇÕES DE UTILIZAÇÃO DO TRABALHO POR TERCEIROS

Este é um trabalho académico que pode ser utilizado por terceiros desde que respeitadas as regras e boas práticas internacionalmente aceites, no que concerne aos direitos de autor e direitos conexos.

Assim, o presente trabalho pode ser utilizado nos termos previstos na licença abaixo indicada.

Caso o utilizador necessite de permissão para poder fazer um uso do trabalho em condições não previstas no licenciamento indicado, deverá contactar o autor, através do RepositóriUM da Universidade do Minho.

Licença concedida aos utilizadores deste trabalho

Atribuição-NãoComercial

CC BY-NC

https://creativecommons.org/licenses/by-nc/4.0/

AGRADECIMENTOS

Com o fim de mais uma etapa na minha vida gostaria de deixar a minha gratidão a todos que tornaram este trabalho possível.

Primeiramente, quero agradecer ao professor José Teixeira por ter aceitado ser meu orientador, pela sua disponibilidade e pelo seu auxílio.

Quero agradecer à Joana Laranjeira e à Allmicroalgae pela oportunidade e disponibilidade de um estágio que me enriqueceu não só a nível profissional, mas também pessoal.

Um enorme obrigada à Maria Soares que me acompanhou em todos os passos desta dissertação e me ensinou praticamente tudo o que sei sobre produção de microalgas. Obrigada pela disponibilidade e apoio.

Um enorme obrigada ao Pedro Cunha, à Inês Guerra, à Rita Pires, ao Rachid Évora e ao Nuno Fernandes por todos os momentos passados na casa 70 e por terem ajudado imenso no meu período de adaptação. Aos da casa 42, Gonçalo Espírito Santo e Pedro Quelhas, também deixo o meu obrigada por tudo. Às restantes estagiárias, Diana Santos, Mafalda Galvão e Carolina Vala, quero, também, deixar o meu obrigada.

Quero ainda deixar o meu obrigada a todo o restante pessoal da UID, Joana Fonseca, Joana Teles, Nádia Correia, Helena Cardoso e Margarida Costa, e a todo o pessoal da UPM, Joana Ribeiro, Inês Pedro, Adriana Machado e Ana Barros, por todos os momentos e por todas as ajudas e ensinamentos. Deixo ainda o meu obrigada a todo o restante pessoal da Allmicroalgae.

Um enorme obrigada à minha família, em particular à minha mãe, ao meu pai e à minha irmã por sempre me apoiarem e, ainda, à minha sobrinha por nunca me deixar trabalhar. Um enorme obrigada aos meus amigos que fizeram que toda esta fase da minha vida fosse um pouco mais fácil e descontraída. Agradeço, ainda, à Lenka por todo o apoio, ajuda, motivação e descontração.

STATEMENT OF INTEGRITY

I hereby declare having conducted this academic work with integrity. I confirm that I have not used plagiarism or any form of undue use of information or falsification of results along the process leading to its elaboration.

I further declare that I have fully acknowledged the Code of Ethical Conduct of the University of Minho.

RESUMO - SET-UP E OTIMIZAÇÃO DE UM FOTOBIORREATOR À ESCALA PILOTO PARA CRESCIMENTO AUTOTRÓFICO DE MICROALGAS

Diferentes tipos de biorreatores podem ser utilizados para cultivar microalgas, apresentado vantagens e desvantagens, principalmente relacionadas com a esterilidade, operação, produtividade, qualidade do produto e custos. Neste trabalho, um fotobiorreator de coluna de bolhas foi testado e modificado. Múltiplos ensaios foram realizados nos fotobiorreatores de coluna de bolhas de 60 L cultivando *Phaeodactylum tricornutum*, que incluíram ajustes no design e operação do reator, nomeadamente a adição de um segundo difusor de ar, um controlador de pH e um sistema de luzes. A adição de um difusor de ar e um controlador de pH melhorou o arejamento no reator e proporcionou a regularização do pH, respetivamente. Estas mudanças refletiram um aumento de 18 % e 5 % na produtividade e taxa de crescimento específico máximas, respetivamente. Três sistemas de luz foram também adicionados e comparados. O sistema com luzes amarelas instaladas na parte de trás do reator proporcionou um aumento geral de 2,9 vezes na produtividade máxima; os outros dois sistemas instalados na parte da frente e de trás do reator, com luzes brancas e o outro amarelas, proporcionaram um aumento de 3,7 vezes e 1,9 vezes na produtividade máxima, respetivamente.

Adicionalmente, o fotobiorreator de coluna de bolhas foi comparado com outros dois sistemas de cultivo, balões de 5 L e fotobioreactores de painéis planos de 70 L, a fim de perceber e otimizar o processo de scale-up autotrófico da Allmicroalgae. O sistema de coluna de bolhas apresentou produtividades areal e volumétrica máximas, de 147,33 ± 43,99 g m^{-2} d^{-1} e 0,25 ± 0,08 g L^{-1} d^{-1}, respetivamente, estatisticamente mais elevadas. Em termos de perfis bioquímicos, foi obtido um teor em proteína estatisticamente mais alto em balões e estatisticamente mais baixo em carotenoides totais em painéis planos. Ao comparar os três sistemas sob o mesmo volume (60 L), a área ocupada por doze balões foi quase 11 vezes superior do que uma coluna de bolhas. A mão-de-obra foi reduzida 2,5 vezes substituindo os balões pelo sistema de coluna de bolhas. Por último, o uso de plástico foi reduzido ao mudar de painéis planos para colunas de bolha, resultando numa redução da pegada ecológica geral. Em conclusão, o processo autotrófico de scale-up, em relação à etapa com um sistema de 60 L, seria melhorado com a adição de um sistema de coluna de bolhas, em relação à produtividade, área ocupada, mão-de-obra e resíduos.

Palavras-chave: Fotobioreactor de coluna de bolhas, optimização operacional, *Phaeodactylum tricornutum*, produtividade, taxa específica de crescimento.

ABSTRACT - SET-UP AND OPTIMIZATION OF A PILOT-SCALE PHOTOBIOREACTOR FOR AUTOTROPHIC MICROALGAE GROWTH

Microalgae can be grown using different types of photobioreactors. All photobioreactors present distinct advantages and disadvantages, specially related to sterility, operation, productivity, product quality, and costs. In this work, a bubble column photobioreactor was tested and modified to reach an optimized state. Therefore, multiple trials using *Phaeodactylum tricornutum* were conducted in the 60 L bubble column photobioreactors alongside technical adjustments on its design and operation, i.e., the addition of a second air diffuser, a pH controller, and a light system. The addition of a sparger and a pH controller improved aeration and provided pH regulation, respectively. These changes provided an increase of 18 % and 5 % in maximum productivity and specific growth rate, respectively. Three light systems were also added and compared. A light system with yellow lights installed in the back of the reactor provided an overall 2.9-fold increase in maximum productivity; the other two light systems installed in the front and back of the reactor, one with white and the other with yellow lights, provided an increase of 3.7-fold and 1.9-fold in maximum productivity, respectively.

The bubble column PBR system was also compared with other two in-house systems, a 5 L balloon reactor, and a 70 L flat panel PBR system. The bubble column system presented a statistically higher maximum areal productivity of 147.33 ± 43.99 g m^{-2} d^{-1} and maximum volumetric productivity of 0.25 ± 0.08 g L^{-1} d^{-1}. In terms of biochemical profiles, statistically higher protein content in balloons was obtained and statistically lower total carotenoid levels were presented in flat panels. When comparing the three systems under the same volume (60 L), the area occupied by twelve balloons was almost 11-fold higher than that of one bubble column. Labor work was over 2.5-fold higher than that of the bubble column or the flat panel when twelve balloon reactors were used. Lastly, plastic use was reduced when changing from flat panels to bubble columns, resulting in a reduction of overall ecological footprint. In conclusion, the scale-up autotrophic process regarding a step with a 60 L system, would be improved with the addition of a bubble column regarding occupied area, labor work, and waste.

Keywords: Bubble column photobioreactor, operation optimization, *Phaeodactylum tricornutum*, productivity, specific growth rate.

CONTENTS

LIST OF FIGURES

LIST OF TABLES

1 INTRODUCTION

1.1 MICROALGAE

1.1.1 GENERAL OVERVIEW

Microalgae are a diverse group that includes eukaryotic or prokaryotic photosynthetic microscopic organisms [1]. Due to their unicellular or simple multicellular structure, they can develop quickly and survive in harsh environments [1]. They are most commonly found in freshwater, brackish, marine, and hyper-saline water, but they can also grow well in moist soils and rocks [2, 3].

Over 50 000 species of microalgae are known to exist but only about 30 000 have been studied, analyzed, and classified [1, 2]. They can range in size from 0.5—200 μm [4]. The diatoms (Bacillariophyceae), green algae (Chlorophyceae), and golden algae (Chrysophyceae) are the three most abundant microalgae families [5].

Microalgae are organisms that produce O_2 as a byproduct of their photosynthesis [6]. In order to incorporate atmospheric CO_2 into proteins, lipids, and carbohydrates, phototrophic microalgae need light and nutrients (nitrogen, phosphorus, minerals) [7]. Microalgae's high photosynthetic yield and efficiency make them extremely capable of capturing large amounts of carbon dioxide [6].

Microalgae present a wide range of applications and are an excellent alternative to land crops due to their high turnover rates [6]. The photosynthetic process of these organisms allow CO_2 (an industrial byproduct), and nitrogen and phosphorus in wastewater treatment systems to be fixed and recycled which results in environmental benefits by their mitigation [8].

1.1.2 APPLICATIONS

Microalgal biomass contains a diverse range of biologically active substances, including proteins, polyunsaturated fatty acids (PUFAs), pigments, vitamins, and minerals, as well as extracellular compounds such as oligosaccharides [3]. It can be used to produce high-value bioproducts for food, pharmaceuticals, fine chemicals, nutraceuticals, animal feed, pigment extraction and cosmetics applications [8]. Microalgae are also known as potential bioresources for other applications, such as wastewater treatment, biofuels, carbon dioxide biosequestration, etc. [9]. They are one of the most promising feedstocks for chemical and biofuel processing that could represent a sustainable and renewable energy source with potentially lower environmental impact [7, 8]. Compared to other biofuel feedstocks, for instance, soybean crops, microalgae represent a far higher production yield, fewer area of implementation hence reducing the demand in regards to arable soil compared to soil demand of plants meant for human consumption [8, 10]. Nevertheless, for microalgae to compete in the bioenergy

market, their production rate and costs have to be to improved [8]. On the other hand, some microalgae organisms have been found capable of producing biomaterials including biocompatible and biodegradable bioplastics [11].

Macroalgae have been used as human food for thousands of years [12]. Far more recently, microalgae are also being used as sources of health-promoting nutritional supplements including antioxidants [12]. Research has demonstrated that microalgae can present health benefits due to their anticancer, anti-inflammatory, antioxidant, antimicrobial, anti-obesity, and hypocholesterolemic properties [3].

Despite microalgae presenting numerous applications and benefits, it is still difficult to reach commercial level due to a variety of constraints [3]. Their production presents a higher cost than some alternatives obtained via chemical synthesis, direct metabolism by fungi, bacteria other microorganisms or even extractions from fossil raw materials [3].

Worldwide, the microalgae market size is still very limited [3]. It began in Japan in the 1960s, with *Chlorella* being the first organism to be targeted [13]. In 2017, microalgae's market value was about €5.7 billion, making the most profit with the health food industry, which accounted for around €2.2 billion [13]. Microalgae annual production was estimated to be around 7.5 million tonnes at the time [13].

1.1.3 FACTORS AFFECTING MICROALGAL GROWTH

Microalgae's growth, the quality of their biomass, the production rate, and their downstream processing can be affected by a vast number of factors [14]. Temperature, light, the availability of macro and micronutrients, and pH can be considered the main factors affecting the growth of microalgal cultures [15]. In addition, salinity and gas exchange should be taken into consideration as well [15].

1.1.3.1 TEMPERATURE

Temperature has a strong influence on the physiological and morphological responses of microalgal growth [15]. As the temperature increases, the biomass productivity generally grows exponentially until the optimum temperature is reached [16–18]. Even though high temperatures increase CO_2 fixation, they also act as an inhibitor factor for the respiration metabolism and photosynthetic proteins by disturbing the cells' energy balance [15]. Temperatures above optimal or sudden changes in temperature lead to the reduction of algal growth rate, or even death of algae cells [17, 18].

Every species has its optimal temperature but commonly varies between 28 and 35 °C for most microalgae [15–17]. In outdoor cultivation, the temperature is strongly determined by atmospheric temperature, sun light and humidity [18]. In closed systems, the temperature of the culture can be

controlled by using water sprinklers, immersing the reactor in cooling pools or placing it inside a greenhouse [16].

1.1.3.2 LIGHT

The availability and intensity of light are one of the main parameters to take into consideration in algae cultivation [16, 18]. It is an essential energy source for phototrophic microalgae [18]. Different light intensities can affect photosynthesis and lead to different biochemical compositions as well as biomass yield [15].

The increase of light intensity leads to the increase of photosynthesis, assuming there is no nutrient limitation [16–18]. However, this only occurs until the maximum growth rate of the species is achieved, at the light saturation point [16–18]. When this point is reached, increasing the light intensity will not increase the growth rate, but on the contrary, it can lead to photoinhibition, resulting in cell damage or even death, thereby reducing the photosynthetic rate and productivity [16–18]. Generally, the optimal light intensity is about 200 up to 400 μmol $m^{-2} s^{-1}$ for most microalgae species, even though some species have it as 100 μmol $m^{-2} s^{-1}$ [15].

With cell concentration increase, the light available is mostly absorbed by the cells close to the surface, leaving the rest in the dark, creating self and mutual shading effects [17, 18]. Furthermore, this can result in light saturation and inhibition on the top layers' cells [18]. However, this problem can be minimized by shortening the light path and providing good mixing to reduce mutual shading and create the circulation of the cells between light and dark zones [18].

According to Lambert-Beer's law (equation 1), the light that penetrates through the culture, gets attenuated by it [15].

$$I(l) = I_0 \exp(-\sigma X l) \quad (1)$$

Where $I(l)$ is the final light intensity after going through the distance l, I_0 is the initial light intensity, σ is the extinction coefficient and X is the concentration of the culture [15].

Halogen, fluorescent, high-intensity discharge lamps, light-emitting diodes (LEDs), or incandescent bulbs can all be used as an artificial light source for cultivations [11]. For algal production, the use of fluorescent and LED lights is predominating [11]. However, the use of LED lights has been identified to be a better option than fluorescent tubes [15]. LEDs only emits spectrum that matches the photosynthetic action spectrum of algae and ineffective frequencies are eliminated [11]. Additionally, their production of heat is the lowest and their lifespan is the longest [11].

1.1.3.3 NUTRIENTS

Indispensable components for microalgal growth are macronutrients, vitamins, and trace elements [15]. Literature usually refers to fixed values of the Redfield C:N:P ratio that is 106:16:1 [15]. However, in practice, the composition of the cultivation media is often altered to suit the metabolic needs of microalgae in different environmental conditions [15].

The predominant element that constitutes around 65 % of biomass dry weight in the majority of microbial species is carbon [15]. However, there is a strict correlation between the increase of carbon and the presence of other nutrients like phosphorus and nitrogen [15]. Carbon is mainly fixed in microalgal cells in an inorganic form through photosynthesis and its form is dependent on the pH of the environment [15]. Values of pH that are lower than 6.5 favor H_2CO_3, range of 6.5 to 10 is dominated by the form HCO_3^-, and CO_3^{2-} is predominant in solutions with pH higher than 10 [15].

CO_2 can be supplied as gas, but the fixation is conditioned by critical parameters such as its solubility and mass transfer rate which is affected by specific contact area and the concentration gradient of the phases [15]. Spargers with CO_2-rich gases are used industrially, which have different solubility depending on the pH – the higher the pH, the faster the mass transfer of CO_2 [15]. During microalgae cultivation, the cost of supplying CO_2 corresponds up to 50 % of the biomass production [15]. Flue gases from coal-fired or cement production plants that consists of 10 % up to 25 % of CO_2 represent a more cost-effective option [15].

The second most significant element that constitutes about 1 % up to 14 % of microalgal dry weight is nitrogen [15]. It is fundamental to biochemical compounds that form DNA, RNA, proteins, and pigments – chlorophylls and phytocyanin [15]. Inorganic nitrogen is provided in NO_3^-, NO_2^-, NO, and NH_4^+ form; organic form is supplied as urea or amino acids [15].

Phosphorus is another microalgal limiting nutrient and represents 0.05 % up to 3.30 % of the biomass [15]. Factors that influence the phosphorus uptake rate consist of available light, temperature, pH, ionic strength, and available cations (K^+, Na^+, Mg^{2+}) that promote phosphate precipitation [15]. Microalgae can be used to treat wastewater and to reduce the amount of phosphorus by accumulating intracellular phosphorus in a form of polyphosphate granules [15].

Micronutrients required for microalgae cultivation include magnesium for enzyme activation and participation in photosynthesis (0.35 % to 0.70 %); sulfur for cell and metabolites structure (0.15 % to 1.60 %); calcium for cell division and morphogenesis (0.1 % to 1.4 %, or up to 8 %), and iron for fundamental enzymatic processes [15].

1.1.3.4 pH

The pH of the culture regulates the uptake of ions and inorganic carbon availability, enzymatic activity, ammonia toxicity and affects the algal growth and metabolism [15, 17].

Similar to the other factors, each species has a certain pH range that leads to optimal growth [16]. Saltwater microalgae species tend to have a pH range of 7.9 up to 8.3, whereas freshwater ones are more likely to have a pH range of 6.0 up to 8.0 [15]. Furthermore, most species are sensitive to pH values above and below their optimal range, which can lead to biomass productivity decrease [15–17].

In closed cultivation systems, the rising of the pH, which can go as high as 10, can be controlled with an automated CO_2 injection system or by adding inorganic or organic acids [15, 16]. The high pH stress can influence the metabolism of the cell and trigger lipid accumulation, for instance [15]. In addition, CO_2 concentration appears to be crucial in order to control the pH and to maintain the carbon balance [15].

1.1.4 *PHAEODACTYLUM TRICORNUTUM*

Diatoms are unicellular photoautotrophic microalgae that play a major role in the global ecosystem [19, 20]. They generate more than 20 % of the oxygen produced on earth, provide approximately half of the marine primary food, engage in the biogeochemical cycling of dissolved silicates by integrating them into their cell walls, and are one of the main contributors to global carbon fixation [19, 20].

Diatoms have gained increasing attention due to their numerous practical applications in the pharmaceutical, cosmetic and food sectors as a natural source of polyunsaturated fatty acids, pigments, and antioxidants [19, 20]. Furthermore, they are also used as expression systems for recombinant proteins or biomaterials [20]. Nevertheless, their greatest potential is likely to lie in biofuel production, considering that the scarcity of fossil fuels keeps increasing [20].

Phaeodactylum tricornutum is a model diatom species and its genome has been fully sequenced and is publicly available [19, 21]. It has been largely reported as a fast growing microalga with high carbon sequestration capacity and viability for large-scale cultivation [21, 22].

Phaeodactylum tricornutum has three main morphotypes, namely fusiform, triradiate and oval, that help the microalgae adapt to different environments (Figure 1) [19]. Fusiform and triradiate cells adapt better in more dynamic growth conditions while the oval cells acclimate better to the benthic environment because they have better sedimentation and surface adhesion [19]. Furthermore, under stressful conditions, fusiform and triradiate cells turn into oval cells, whereas under favorable growth conditions, oval cells transform into fusiform and triradiate morphotypes [19].

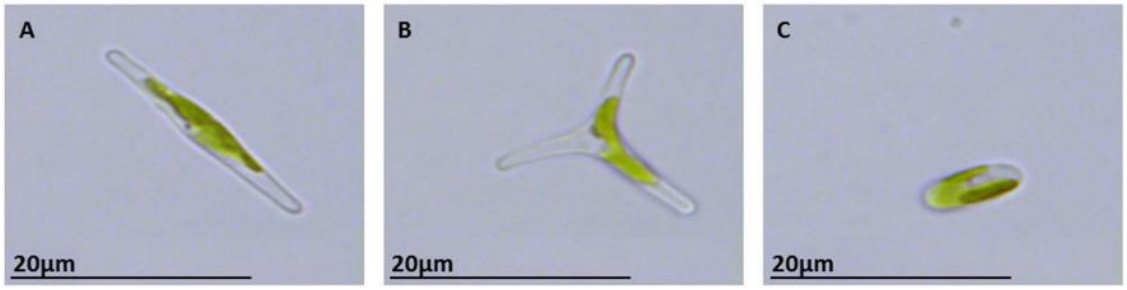

Figure 1: Microscopic view of *Phaeodactylum tricornutum* in A) fusiform morphotype, B) triradiate morphotype, and C) oval morphotype [23].

One of these microalgae features is the interesting lipid profile, having around 30 to 45 % of polyunsaturated fatty acids (PUFA) from the total fatty acids, of which eicosapentaenoic acid (EPA) is the main one, accounting for 20 to 40 % of the total fatty acids of *Phaeodactylum tricornutum* [22, 24]. EPA is an important fatty acid for the human metabolism that helps to maintain blood lipid balance, decreases triglyceride levels in the blood, i.e., prevents hypertriglyceridemia, and has anti-inflammatory properties [22, 24]. However, salinity is an important parameter to pay attention to when cultivating this microalga because it is known to alter its biochemical composition, particularly, the levels of EPA [22].

Silicon is known as a key nutrient for diatoms and can be a growth-limiting factor since the silicification and silicate transport are related to the cell cycle, however, it is often estimated that silicate has little impact on *Phaeodactylum tricornutum* [19].

1.2 MICROALGAE METABOLISM

Whereas the capacity to perform photosynthesis is unquestionably a main characteristic of microalgae, they can also be grown as chemoorganotrophs, also known as heterotrophs, or even mixotrophs [6]. Greater productivity can be achieved in certain cases by using these cultivation methods [6].

1.2.1 AUTOTROPHIC CULTIVATION

Nowadays, autotrophic growth is the most commonly used method of cultivating microalgae [15]. Since all microalgae are photosynthetic organisms, they are grown in naturally or artificially illuminated conditions [25]. This method of producing these microorganisms can be especially advantageous due to the use of natural sunlight as the energy source [6]. Under this type of cultivation, microalgae cells harvest light energy and use CO_2 as a carbon source [6, 14]. The key goal and limiting factor of cultivation is to introduce enough light to promote high cell density cultures [6, 14].

1.2.2 HETEROTROPHIC CULTIVATION

Compared with autotrophy, heterotrophy does not require light and can be maintained in total darkness [6, 15]. However, the use of microalgae's heterotrophic growth potential is limited to a few species [25]. This method of cultivation provides organic compounds dissolved in the culture media as a carbon and an energy source [6, 14]. Although this obviates the need for lighting, it increases the expense of the organic substrates [6]. However, compared to autotrophy, heterotrophy presents a higher cell growth rate, increased biomass and lipid accumulation, which leads to reduction of cost per gram [26]. Since heterotrophy presents a higher lipid accumulation yield, it is considered to be a better method for biodiesel production [26].

On the other hand, as mentioned above, the limited amount of heterotrophic microalgal species and the increasing energy costs are the major limitations of this method [25]. This method of cultivation also increase the possibility of growth inhibition caused by the excess of added organic substrate, the inability to generate light-induced metabolites, and the growing microalga can rapidly be overturned if contaminated by competitor microorganisms [25].

1.2.3 MIXOTROPHIC CULTIVATION

Mixotrophy, also called as photolithotrophic heterotrophy, can be extremely beneficial for microalgae, distinctively when light availability is low and CO_2 is subsaturated [6]. Mixotrophic organisms has attributes of both heterotrophic and autotrophic metabolisms [27]. They are able to use both organic compounds and CO_2 as a carbon source to synthesize cells [27]. They simultaneously respirate and release CO_2 that is immediately captured and used again when light intensity is sufficient enough [27]. This means that mixotrophy obtains energy from respiration similarly to heterotrophy, i.e., catabolism of organic compounds, and from photosynthesis similarly to autotrophy, i.e., conversion of light energy to chemical energy [27]. This method is better when combined with the dark-light cycle, which helps the microalgae to grow at their optimum autotrophic and heterotrophic conditions [26]. Microalgae grow heterotrophically with organic carbon, increase the growth rate, biomass and lipid content, but also consume inorganic carbon and produce oxygen through photosynthesis [26]. Therefore, it can lead to a better biomass and lipid content, since mixotrophy combines the advantages of both methods [26]. Some species that are able to alter between heterotrophy and autotrophy based on the availability of light and organic substrate are called amphitrophic organisms [27].

1.3 MICROALGAE CULTIVATION SYSTEMS

Nowadays, the most cultivated microalgae are autotrophic species [25], therefore this chapter will be focused on photobioreactors targeted on the cultivation of autotrophic organisms.

Production at the maximal capacity of any microalgae strain is possible if they are provided with the optimal conditions. That is irradiance, temperature, pH/CO_2, dissolved oxygen as well as the remaining nutrient's availability [28]. After the identification of a strain of interest, design and optimization of the photobioreactor follows [28]. Photobioreactor (PBR) is a designated vessel specifically designed for the controlled production of biomass [29], to provide optimal conditions that the microalgae strains requires at minimal cost [28].

The capacity of any photobioreactor to provide said optimal conditions are conditioned by its geometry, fluid dynamics, mass and heat transfer capacity [28]. The design of the PBR must also consider the prevalent environmental conditions specific to the selected location, e.g., solar radiation and temperature throughout the year as well as during diurnal cycles [28].

Many PBR designs have been purposed and can be generally differentiated into open and closed/partially enclosed systems [6, 16, 30]. Examples of open cultivation systems are unstirred, raceway, paddlewheel open ponds [15]. Closed systems can be classified into different types, including tubular, column, membrane, and flat panel photobioreactors [15]. 'Photobioreactor' is increasingly used as a narrower term for a closed cultivation system [31].

1.3.1 OPEN CULTIVATION SYSTEMS

Most presumably, the very first photobioreactors were in a form of natural bodies of water where algae grew and were later developed into man-made ponds [30]. Open cultivation systems can be either stirred or unstirred, in a form of tanks, e.g., shallow large ponds, circular, or raceway tanks (Figure 2) [32]. They are the most common solution for low-cost mass cultivation, as they require low capital investments and are typically built in concrete or compacted ground [6, 15, 16]. The simplest and most cost-effective are unstirred open ponds, however, they are also the most ineffective in terms of biomass production [32]. Nowadays, more than 80 % of global algal biomass is obtained from raceway ponds [15]. Some microbial interactions can have mutual benefits, for instance, bacteria and microalgal symbiosis, which provides extracellular products [15].

However, not all microalgae species can be successfully grown in open ponds since there are some disadvantages related to these systems [6]. They require a large amount of water given that present high evaporative losses, and are exposed to microbial contamination [6, 15, 16, 32, 33]. Algal productivity is significantly affected by variations of diurnal temperature, which are dependent on the location of the

production site and weather conditions [15, 33]. Pond depth is another factor that needs to be considered since light penetration is more efficient at lower depth, by which the surface to volume (S/V) ratio is increased as well [15]. Depth of raceway ponds should range from 0.2–0.3 m [15, 32].

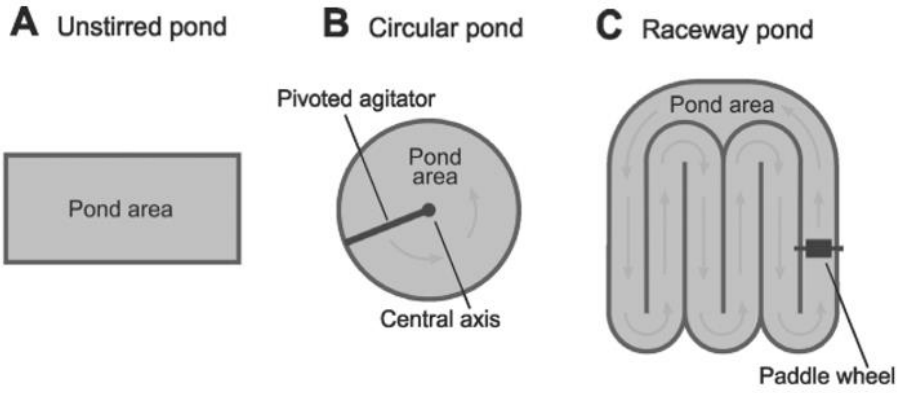

Figure 2: Schematics of different types of open cultivation systems. A) Unstirred pond. B) Circular pond. C) Raceway pond. [32]

1.3.2 CLOSED CULTIVATION SYSTEMS

Even though closed or nearly closed photobioreactors have been designed to overcome the disadvantages of using open ponds [25], they present some limitations, including being more prone to biofilm formation, leading to oxygen accumulation, which can be toxic to photosynthetic growth. Also can constrain light to penetrate the culture [15, 16]. The operation of closed PBRs is more complex than that of open ponds and needs to take into consideration potential overheating and cell damage due to shear stress [34]. The capital investment for closed cultivation systems are higher than those of open systems, namely due to their installation, maintenance, and operation [25, 31].

Even though it is more expensive to operate and it is technically more difficult to scale up the production, the productivity of the closed cultivation system, however, is higher than that of any open system on a routine basis [32]. The use of this system eliminates the loss of water by evaporation, significantly lowers the possibility of microbial contamination [31]. Moreover, closed systems allow for controlled cultivation conditions, such as temperature, nutrients, CO_2, and dissolved oxygen that can result in more reproducible cultivation conditions [32, 35].

One of the key goals for future photobioreactors is to improve operational approaches to control rate-limiting parameters of cultivation growth, including temperature, pH, and gas diffusion [25]. Due to the benefits associated with these cultivation systems, the demand and sales of closed PBRs are expected to increase by 2024 [15].

An abundant number of PBR types and designs have been introduced to the industry, and all of them can be essentially assigned to one of the three following categories based on their basic geometry: i) vertical column (cylindrical) type includes all tank reactors, e.g., bubble column, airlift, annular, and stirred tank reactors [29, 31]. Another type, ii) flat panels offer cuboid and hemispherical shapes [28, 31]. Lastly, iii) tubular PBRs comprise all plug flow tubular reactors with tubes in straight, conical, and helical structure systems [31]. Some of these designs will be discussed in the following subsections.

1.3.2.1 TRANSPARENT STIRRED TANK PHOTOBIOREACTORS

For algal cultivation, the redesign of a glass fermenter, which is typical for biotechnological use, is the simplest approach to obtain a stirred tank reactor (STR-type) (Figure 3) [31]. The majority of the reactor designs contain a basic transparent vessel that is generally equipped with an external light source, e.g., tubular fluorescence or halogen lamps [36, 37]. This means that the supplied light only reaches the outer regions of the culture, which is a major disadvantage of this type, hence, a stirring system is needed to ensure good performance which is at the expense of higher energy cost [31, 36, 37]. Additionally, the microalgae photosynthetic efficiency is reduced by a low S/V ratio which causes substandard light penetration [36, 37]. This is also the reason why this system is only used for laboratory purposes and has never secured its place on the industrial level [31, 36].

The STR-type PBRs can operate in both continuous and discontinuous regimes and only 70 % to 80 % of its capacity should be filled with the culture to allow easy gas exchange in the remaining space [31, 37].

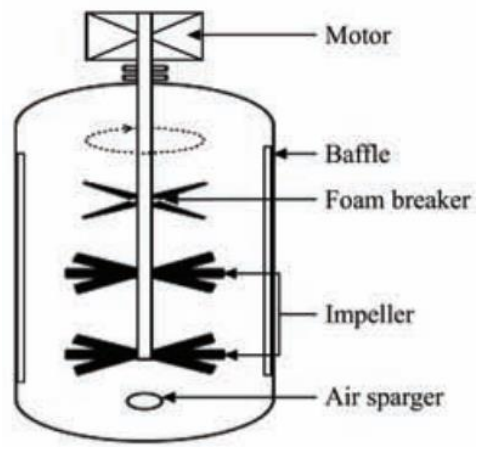

Figure 3: Schematics of a stirred tank photobioreactor [37].

1.3.2.2 TUBULAR PHOTOBIOREACTORS

The first developed model of closed reactors for microalgae production was a tubular photobioreactor (Figure 4) [36]. They are usually made of glass or different transparent plastic material [36]. Circulation and aeration are ensured by the addition of air pumps or airlift systems [31]. These

PBRs are usually used for outdoor cultivation, and the flow characteristics, as well as illumination angle, is greatly dependent on the geometry and positioning of the tubes, which can be horizontal, vertical, angular and helical, creating walls, panels or helices [15, 36]. They have to be consciously constructed in order to enhance sunlight capture [15, 36].

Horizontal tubular PBRs can occupy a vast area of land because although they can long (up to 100 m), their diameters cannot exceed 60 mm nor be less than 10 mm wide, to avoid interfering with light permeability [15, 36]. Nowadays, the horizontal tubular reactor system is the most popular among the many variations of tubular PBRs, and it is characterized by a high S/V ratio (up to 100/1), which maximizes the time the microalgae are exposed to light [31].

One of the drawbacks of this system is higher energy consumption in comparison to flat panels and bubble column PBRs [15] because the culture needs to be pumped steadily into the reactor, where it circulates inside the tubes and is recycled back to the reservoir [36]. The flow regime should always be maintained highly turbulent in order to prevent microalgae sedimentation and provide sufficient exposure to light [36]. They are prone to biofilm formation inside the tubes [15]. Furthermore, due to small diameters and high light exposure, high temperatures in the culture can be reached [15]. Hence, due to scarce separation of oxygen from the culture broth, concentration of dissolved oxygen increases resulting in possible growth inhibition [31].

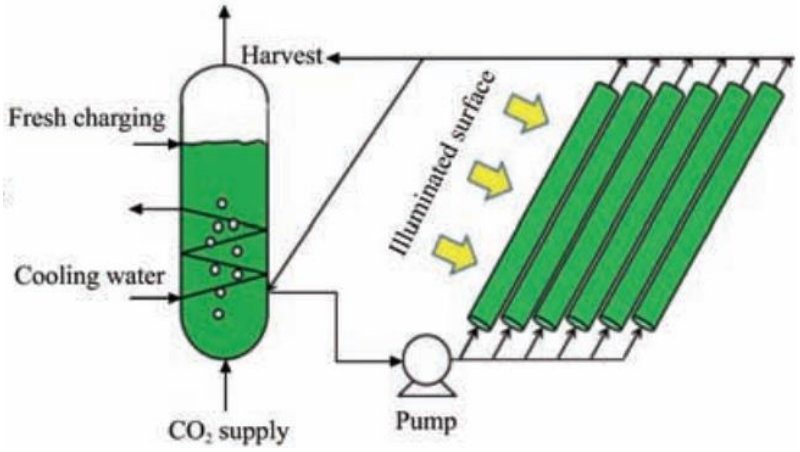

Figure 4: Schematics of a tubular photobioreactor [37].

1.3.2.3 FLAT PANEL PHOTOBIOREACTORS

Another common type of photobioreactor is the flat panel (Figure 5) [36]. Typically, the materials used for their production are glass, polycarbonate, or other transparent or semi-transparent material and have a cuboid shape [15, 36].

This type of PBR is characterized by its high S/V ratio and is usually placed in a vertical or diagonal position [15, 36]. These photobioreactors present a short light path, which provides great light penetration

[36]. Although this may result in high temperatures, it can be easily controlled by sprinkler systems or submerging a part of the photobioreactor in water [15, 36]. This PBR contains an air sparger inside that creates air bubbles, allowing the culture to mix and circulate properly [15, 36]. Furthermore, providing an adequate amount of carbon dioxide and mixing rate will increase the microalgae biomass productivity while keeping oxygen accumulation at low levels [36]. The design is suitable for the scale-up system due to its flexibility and easy operation [36].

Some disadvantages of these systems are biofouling and the aeration of the system can cause cell stress and subsequent damage [36].

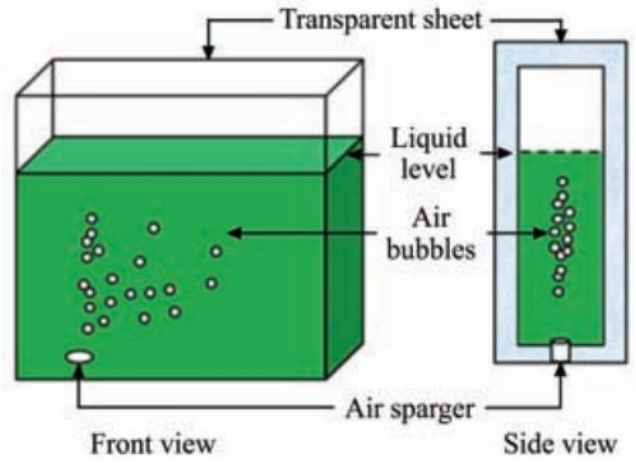

Figure 5: Schematics of a flat panel photobioreactor [37].

1.3.2.4 Column photobioreactors (bubble and airlift)

Column PBRs are vertical cylinder-shaped systems, usually made of glass or plastic (predominantly PE or PMMA) [31]. One of many advantages of this system includes a high level of mass transfer, i.e., import of CO_2 and export of O_2, and low chance of biofouling [31]. Column PBR's construction contains an air diffuser at the bottom creating air bubbles that provide a satisfactory mixing of the microalgae with the culture medium at low shear forces. Additionally it prevents sedimentation, and ensure that the exposure to light is uniform [15, 36]. The surface area of the water and gas phase is increased as the bubbles created are very small, which leads to efficient removal of oxygen produced, and subsequent higher growth rates [36].

Determination of structural features such as the diameter of these vertical tubular photobioreactors must take into consideration factors such as light availability and shading effect. For structural reasons, the height of column PBRs should not exceed 4 m due to the strength and resistance of the used transparent material, since increased height also increases overall volume and pressure [15].

The maximum biomass production obtained in these photobioreactors, along with the operation efficiency, are affected by the morphological features of the algae, the dimensions of the column and the

light intensity [15]. Two types of column PBRs can be differentiated based on aeration mode, bubble column and airlift column (Figure 6) [15, 31, 36].

A major asset of a bubble column PBR is low capital investment [31]. The bubble column is characterized by the absence of any special internal structure, and a sparger at the bottom which ensures agitation by the bubbling of air or it is enriched with CO_2 [31, 36]. Illumination is provided from an external source [31]. Gas flow rate enables liquid mixing causing microalgae cells to move from dark areas (center) to illuminated (outer) zones [36]. This means that the photosynthetic efficiency is highly dependent on the gas flow rate [31]. The S/V ratio of bubble column PBRs is more beneficial than that of stirred tank reactors [31].

The internal structure of an airlift column PBR consists of two interconnected zones, one being the riser zone and the other the downcomer zone [36]. The air bubbles drive the fluid from the smaller tube to the illuminated zone, which provides better cycling between light and dark zones [36]. The airlift column is known to be an enhanced version of the bubble reactor that is cost-effective for the production of various types of microalgae [36].

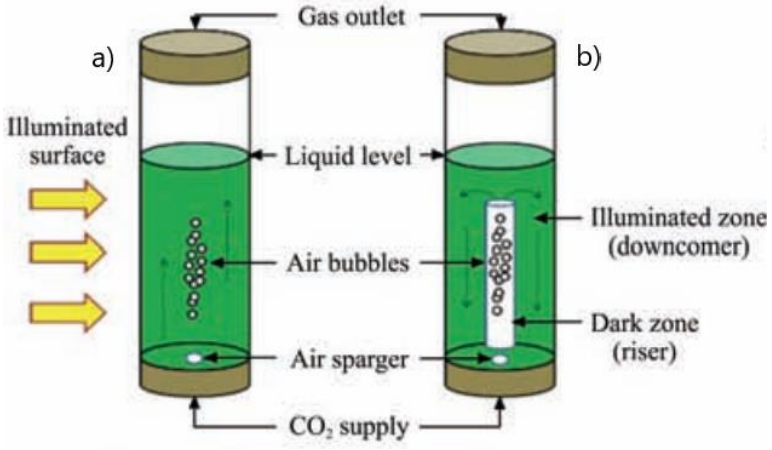

Figure 6: Schematics of a column photobioreactor, a) bubble column, b) airlift column [37].

1.4 OPERATION REGIMES

Bioreactors are commonly operated under one of three regimes, namely batch, continuous and semi-continuous.

1.4.1 BATCH OPERATION REGIME

The batch regime consists of a single inoculation, where the culture and all the necessary nutrients are loaded into a bioreactor [38, 39]. After a growing period and, generally, when a late logarithmic or stationary growth phase is reached, the culture is completely harvested [40, 41].

This regime is frequently used due to its simplicity and adaptability, which does not require much control nor specialized skills, and allows for quick species changes and corrections of system flaws [38, 39]. However, this method is not necessarily the most efficient one [38]. Due to low culture densities during inoculation and high nutrient levels, a long lag phase can occur thus contaminants can sometimes outgrow the culture [38]. Furthermore, the culture is maintained in the bioreactor for a long period, which leads to product variations [38]. In addition, after a batch cycle is completed, the bioreactor requires cleaning and disinfection, leading to an overall longer non-productive time compared to other regimes [38].

1.4.2 CONTINUOUS OPERATION REGIME

In the continuous regime, the bioreactor is being continuously fed, with a culture medium containing all the needed nutrients, with the same flowrate as the excess culture is being simultaneously removed from the vessel [38, 39]. If operated under the optimal dilution rate, this regime allows the culture growth rate to always stay close to the maximum [38].

This regime can be divided into two categories, turbidostat and chemostat [38]. In a turbidostat culture, the cell density is monitored and kept at a pre-set level by an automatic system, by diluting the culture with a fresh medium [38, 41]. In a chemostat culture, the fresh flow of medium is introduced into the culture at a steady and pre-determined rate, keeping a constant growth rate, and not the cell density [38, 41].

In most cases, with this operation regime, higher productivity levels are reached since the culture is maintained near the maximum growth rate, and the quality of the biomass is more predictable [38, 42]. On the other hand, it is a system with higher costs and complexity [38].

1.4.3 SEMI-CONTINUOUS OPERATION REGIME

In the semi-continuous regime, when a mid to late logarithmic growth phase is reached, a proportion of the culture, generally 10 % to 50 %, is harvested and replaced with fresh culture medium [40, 41]. After allowing the remaining culture to regain cell density for 1 to 5 days, the process is repeated [40, 41].

Compared to the batch regime, the semi-continuous system does not waste as much non-productive time for cleaning and disinfection and overall yields more biomass [38, 39].

1.5 ALLMICROALGAE

Allmicroalgae – Natural Products S.A is a Portuguese company located in Leiria, that produces microalgae via autotrophic and heterotrophic cultivation in different culture systems such as tubular photobioreactors, flat panels, open raceways ponds and fermenters in large-scale production [43].

The company first started as a sustainability project from Secil, one of the largest cement companies in Portugal [43]. The project aimed to create a microalgae production plant to fix CO_2 emitted by the cement company, therefore meeting the targets for greenhouse gases reduction set by the European Union [43, 44]. The project started with a Research and Development Department with an emphasis on pilot-scale and laboratory work [43]. The large-scale production of microalgae started in 2013 [43].

The company focuses on optimizing the process and culture conditions to achieve maximum biomass production maintaining a suitable biochemical profile and functional activity of the microalgal biomass. The scale-up process starts in a master cell bank, where strains are cryopreserved. In autotrophy, the culture starts in a lab-scale reactor (balloon or Schott flask) that is later scaled up to a flat panel reactor. The culture is then transferred to a larger system, such as an industrial tubular reactor. In the downstream processing, the culture can be concentrated by membrane filtration, in which biomass is recovered from the liquid culture. The biomass is then pasteurized to reduce its microorganic load thus preserving its biochemical quality for a longer period of time. Then it can be processed by centrifugation to obtain a fresh paste as the final product, or by spray drying to obtain a fine powder. The finished product is then packaged, labeled, and kept in suitable storage [43].

Microalgae solutions are delivered all over the world by Allmicroalgae – Natural Products S.A. Their products serve different fields such as human nutrition, nutraceuticals, animal feed, agriculture, and cosmetics. Allmicroalgae focus on the production of *Chlorella vulgaris*, *Arthrospira platensis* (Spirulina), *Tetraselmis chui*, *Nannochloropsis* sp., *Scenedesmus* sp., *Phaeodactylum tricornutum*, and *Chlorococcum amblystomatis*. Allmicroalgae is certified by the European Organic Production Certification, ISO 22000 and ISO 9001, Halal, Portugal Sou Eu, GMP+FSA, GMP, and Kosher, making the company known for its exceptional quality [43].

Figure 7: Allmicroalgae industrial production plant in Pataias, Leiria [45].

1.6 OBJECTIVES

The main goals of this project were to optimize the design of a bubble column photobioreactor and to optimize the autotrophic scale-up process of the company by introducing the bubble column photobioreactor system. To achieve these goals, the following strategy was outlined:

- Assessment of microalgae growth in bubble column systems with different design features: pH control, lighting, aeration, etc.
- Economical, labor, and ecological comparison of the optimized bubble column PBR to different scale-up systems (balloon reactors, flat panel photobioreactors) in the autotrophic scale-up process.

2 MATERIALS AND METHODS

All the experiments described in this work were performed at Allmicroalgae's facilities between the 1st of March of 2021 and the 21st of October of 2021.

2.1 MICROALGAE STRAIN AND CULTURE MEDIA

For this work, *Phaeodactylum tricornutum* was chosen as an autotrophic species to carry out experiments. Namely strains 0018PA and 0079PN (internal codes) used in this work were obtained from Allmicroalgae's culture collection.

The base medium used for *Phaeodactylum tricornutum* cultivation was the standard saltwater nutrient medium used at Allmicroalgae. This derives from the adjustment of the common Guillard-based medium adjusted to the local water composition. For this work, the base media at a nitrate concentration of 10 mM was supplemented with iron (25 µM), magnesium supplement (Necton, Olhão, Portugal) and sea salt (NaCl). The culture salinity was adjusted to and maintained at 30 g L^{-1} throughout the experiments. An antifoaming agent (10 µL per liter of culture) was added to the culture whenever it was needed.

2.2 OVERALL EXPERIMENTAL OUTLINE

Firstly, a preliminary comparison of four water sources and two *Phaeodactylum tricornutum* strains (0018PA and 0079PN) was carried out to determine which one to use for the following steps of this work.

Secondly, multiple trials under batch operation regime were conducted in the bubble column photobioreactor to evaluate the effect of the operational adjustments (addition of a sparger and a pH controller) on microalgal growth. A trial under a semi-continuous operation regime was conducted in the bubble column PBR to compare with the batch regime. Furthermore, three different external light systems were assessed by comparison of their addition to the bubble column PBR with changed design features.

Lastly, the bubble column PBR was evaluated by its comparison to two other in-house systems (balloon reactors and flat panel photobioreactors) which are both incorporated in the scale-up autotrophic process of the company.

2.2.1 WATER SOURCE FOR CULTIVATION

Four different water sources:

– municipal water (tap),

– softened water (water with calcium and magnesium salts removed),

– demineralized water (purified water),

– process water (water used for manufacturing processes at Allmicroalgae extracted from a local well),

were used to access their composition influence on culture growth. The trial consisted of twelve 5 L balloon reactors (Figure 8) starting at a biomass concentration of approximately 0.02 g L^{-1}. Culture growing in 5 L balloon reactors was used as inoculum.

These bioreactors were kept in constant aeration and pH was kept at the setpoint (approximately 8) by supplementing compressed air with CO_2 when necessary. Air and CO_2 were sterilized by 0.2 µm filters. The temperature was kept between 18 °C and 24 °C. These bioreactors were kept under constant irradiance (24:0 h photoperiod) of approximately 200 µmol of photons m^{-2} s^{-1}. This assay was followed by 32 days in triplicates for each water source. Sampling for optical density analysis was done 3 times a week. Sampling for nitrate concentration and pH analysis was done once a week.

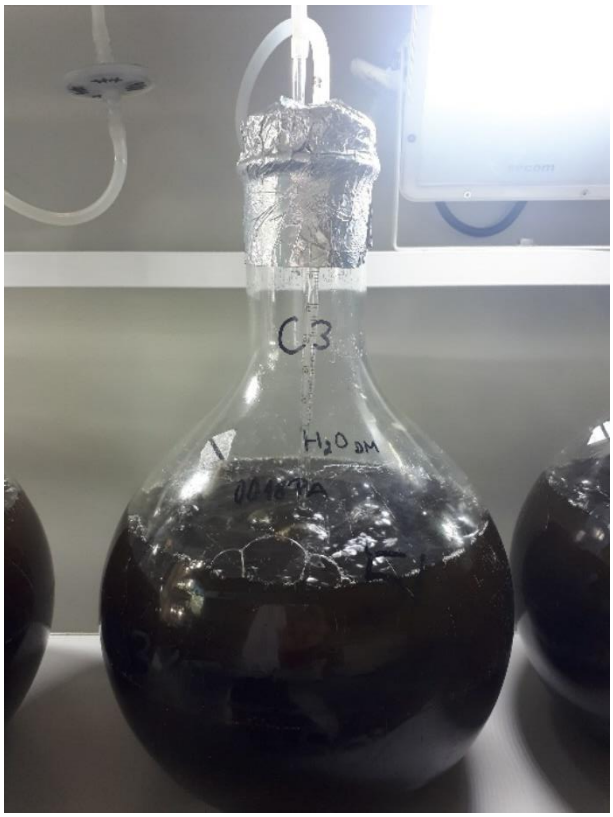

Figure 8: 5 L balloon reactor.

2.2.2 *PHAEODACTYLUM TRICORNUTUM* STRAIN

Two strains (0018PA and 0079PN) of *Phaeodactylum tricornutum* were tested. The initial concentration of approximately 0.35 g L^{-1} was set to start three different cultivation systems: i) 1.5 L balloon reactors, ii) 70 L flat panel PBRs, iii) Algem® lab-scale photobioreactor (version 5.3).

The trial in 1.5 L balloon reactors (Figure 9) was conducted in triplicates for each strain. Culture growing in 1.5 L balloon reactors was used as inoculum. Aeration and pH control, temperature and light conditions were the same as described in Chapter 2.2.1 for 5 L balloon reactors. This assay was followed for 10 days, and sampling for optical density analysis was done every weekday.

Figure 9: 1.5 L balloon reactor.

The trial in 70 L flat panel photobioreactors (Figure 10) was conducted in triplicates for each strain. Culture growing in 5 L balloon reactors was used as inoculum. These photobioreactors were also kept in constant aeration and sterilized by a 0.2 µm filter at the entrance. CO_2 supplementation was adjusted manually when needed. pH was kept between 7.5 and 8.1. The temperature was kept under 26 °C using an irrigation system (only on the first and last day of inoculation). This assay was followed for 4 days. Sampling for optical density analysis was done on the first and last day of cultivation.

In the Algem® lab-scale photobioreactor (version 5.3) (Figure 11), all experimental settings are automatically controlled. Culture growing in 1.5 L balloon reactors was used as inoculum. This system models a wide range of variables for microalgae growth, including lighting and temperature conditions, mixing, aeration, and pH. It features an Algem® software that was designed to recreate the desired conditions and to model monthly light and temperature profiles of a specific place. All conditions are highly controlled by the system, and the human error is eliminated. This software registers the culture optical density, pH, and temperature every hour.

The system contains two separated photobioreactors, with a working volume of 700 mL each, one was inoculated with the 0018PA strain and the other with the 0079PN strain. One replicate was conducted for each strain under the light and temperature conditions in Pataias, Leiria during summer and winter. After setting the conditions, the system was closed, and was opened again at the end of the trial. The optimum pH was set at 8 and CO_2 was pumped automatically. The reactors were kept under

constant aeration. Manual sampling for optical density analysis was done twice, at the beginning and the end of each trial.

Figure 10: 70 L flat panel photobioreactor.

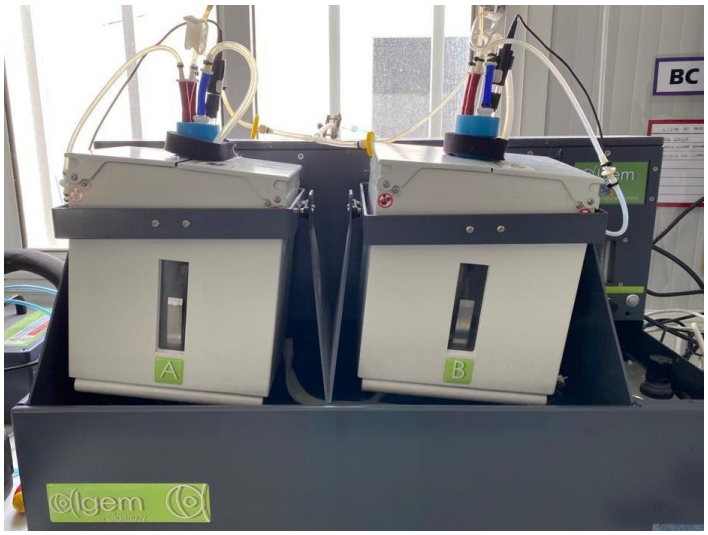

Figure 11: Algem® lab-scale photobioreactor (version 5.3).

2.2.3 BUBBLE COLUMN PBR OPTIMIZATION

2.2.3.1 ADDITION OF AIR DIFFUSER AND PH CONTROLLER

A bubble column PBR designed in-house by Allmicroalgae was altered by the addition of a second air diffuser and a pH controller. The effect of this change was determined by inoculation of both designs (before and after changes) and comparison of microalgal growth. In every trial, culture growing in 5 L balloon reactors was used as inoculum. Sampling for optical density analysis was done 3 to 4 days a week and sampling for nitrates concentration analysis was done once a week.

Before any changes (Figure 12 a)), a bubble column photobioreactor was started with 60 L of working volume and initial biomass concentration of 0.1 g L^{-1} biomass concentration. It was kept in constant aeration by one air diffuser. CO_2 was manually pumped in response to pH changes to a setpoint of 8. Sampling for pH analysis was done twice a day, every weekday, in the morning and in the afternoon. Temperature was kept between 19 °C and 23 °C. The photobioreactor was kept under constant irradiance (24:0 h photoperiod) of approximately 200 µmol of photons m^{-2} s^{-1}. This trial was followed for 17 days.

After adding another sparger and a pH controller (Figure 12 b)), the bubble column photobioreactor was also started with 60 L of working volume and initial biomass concentration of 0.1 g L^{-1}. It was kept in constant aeration by two air diffusers. CO_2 was injected by an automatic system to keep pH bellow 8. When pH levels of 8.05 were reached, the CO_2 valve was automatically opened and closed when the pH was 7.95. The parameters of temperature and light were kept under the same conditions as in the previous trial. This trial was followed for 16 days.

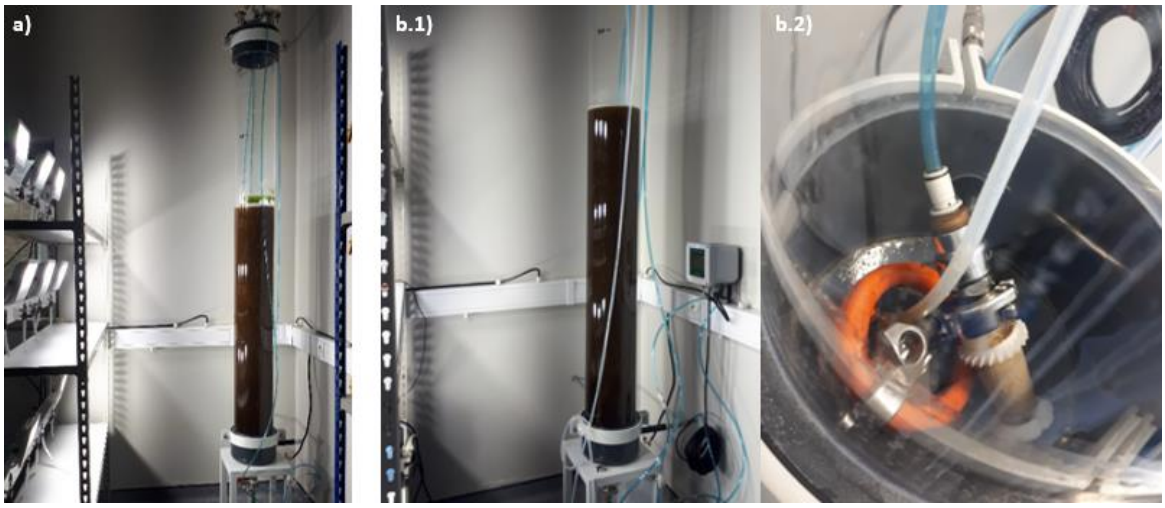

Figure 12: Bubble column photobioreactor a) before any changes, b) after changes, b.1) with a pH controller and a pH sensor installed, b.2) featuring 2 spargers.

2.2.3.2 LIGHT SYSTEM

Three different light systems were installed on the bubble column photobioreactors.

The following experimental procedure for distance (between the reactor to the light system) and light intensity were performed for only one of these light systems. Photon flux density (µmol m^{-2} s^{-1}) of the light was measured using a spectroradiometer, SpectraPen mini (PSI, Photon Systems Instruments, Czech Republic). This parameter was measured in four out of 36 setting stages of light intensity, namely: 9, 18, 27, and 36, which correspond to 25 %, 50 %, 75 %, and 100 % of the total system capacity, respectively. In each stage, the light parameter was measured in three different points of the reactor,

point 1) at the right side of the reactor, 2) at the middle point, closest to the light source, and 3) at the left side, as shown in Figure 13. Furthermore, maximum water temperature inside the reactor was measured at different distances from the surface of the reactor to the lights (on stage 36). Overall, five distances were analyzed (7.5 cm, 11.7 cm, 17.2 cm, 24.0 cm, 27.1 cm).

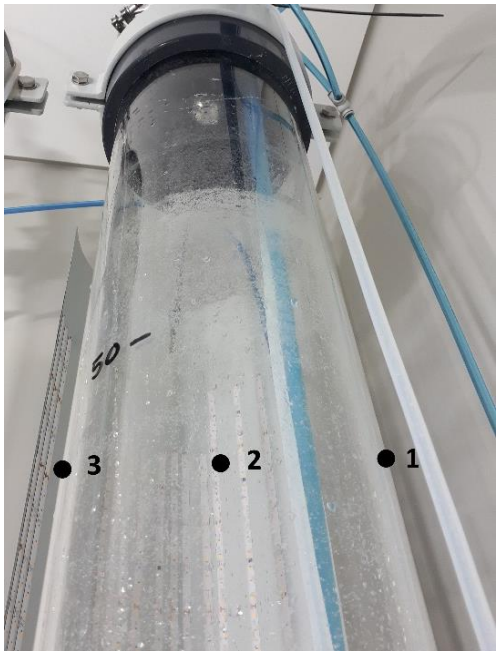

Figure 13: Setpoints on the bubble column photobioreactor where the spectroradiometer was used.

After defining the maximum irradiance possible that doesn't result in an inhibitory temperature increase, three light systems were installed in bubble column PBRs.

The first light system featured a metal sheet installed in the back of the reactor that included 18 lines of yellow LED lights. Second light system featured two metal sheets that included 3 lines of white LED lights, in the front and in the back of the reactor. The third light system was the same as the second system with the exception of having yellow LED lights. In every trial, culture growing in 5 L balloon reactors was used as inoculum. Sampling for optical density analysis was done 3 to 4 days a week and sampling for nitrates concentration analysis was done once a week.

The bubble column with the first light system started with a biomass concentration of 0.4 g L^{-1} and contained 2 air spargers. The bubble columns with the other two light systems started with a biomass concentration of 0.1 g L^{-1} and had only 1 air diffuser. The light systems were kept at a 27.1 cm distance from the closest point of the photobioreactor and under a constant irradiance (24:0 h photoperiod) of approximately 410 µmol of photons m^{-2} s^{-1}. Aeration was kept constant by two spargers, and CO_2 was injected by an automatic system to keep pH bellow 8. When pH levels of 8.05 were reached, the CO_2

valve was automatically opened and closed when the pH was 7.95. Temperature between 21 °C and 25 °C was maintained by a ventilator which was kept under the reactors. The trial was followed for 24 days.

2.2.3.3 Comparison of different operation regimes

A batch cycle was done on the bubble column photobioreactor system. It started with a biomass concentration of 0.1 g L^{-1}. Culture growing in 5 L balloon reactors was used as inoculum. It was kept under constant aeration with 1 sparger. CO_2 was injected by an automatic system to keep pH bellow 8. When pH levels of 8.05 were reached, the CO_2 valve was automatically opened and closed when the pH was 7.95. Temperature was kept between 21 °C and 25 °C and it was regulated by a ventilator that was kept under the reactors. The photobioreactors were kept under constant irradiance (24:0 h photoperiod) of approximately 200 µmol of photons m^{-2} s^{-1}. The trial was followed for 27 days. The batch cycle data collected was analyzed using the Excel Solver Add-In on Windows 10 on the Ruiz growth model Excel sheet [46].

To evaluate the semi-continuous regime, three renovations of 18 L were made every 3 days on the bubble column system. Sampling for optical density was done every weekday, and before and after each renovation.

2.2.3.4 Design

A total of 6 bubble column photobioreactors were installed at the company. One photobioreactor was set in a separate bench while the other five were set in another bench with five holes.

The bubble column PBR system schematics is shown in Figure 14 and Figure 15. One reactor consists of a long tube made of clear acrylic with the height and diameter of approximately 207.1 cm and 19.6 cm, respectively. The reactor is closed on the top and the bottom, which contain inlet and outlet, respectively. At the top, there are four inlets: i) the middle one is connected to an elbow tube and leads to a spray ball; ii) another inlet is to connect the exhaust air filter (Demicap Tetpor and Demicap Propor SG); iii) the third one was used to manually inoculate or to add any required solution during the cycle; iv) the design of the last inlet is different from the other 3 and is used to insert the tube for air and CO_2 inside the reactor. The bottom has one outlet valve, and it is used for taking samples and to connect a hose for harvesting or cleaning purposes.

The tube for air and CO_2 reaches to the bottom of the inside of the reactor where it is connected to the air sparger(s). In one of the 6 reactors, this tube is divided into 2 tubes and is connecter to 2 air spargers. The other 5 reactors consist of 1 sparger only.

Figure 14: Bubble column photobioreactor system 3D design, with height and width measurements (Allmicroalgae designs).

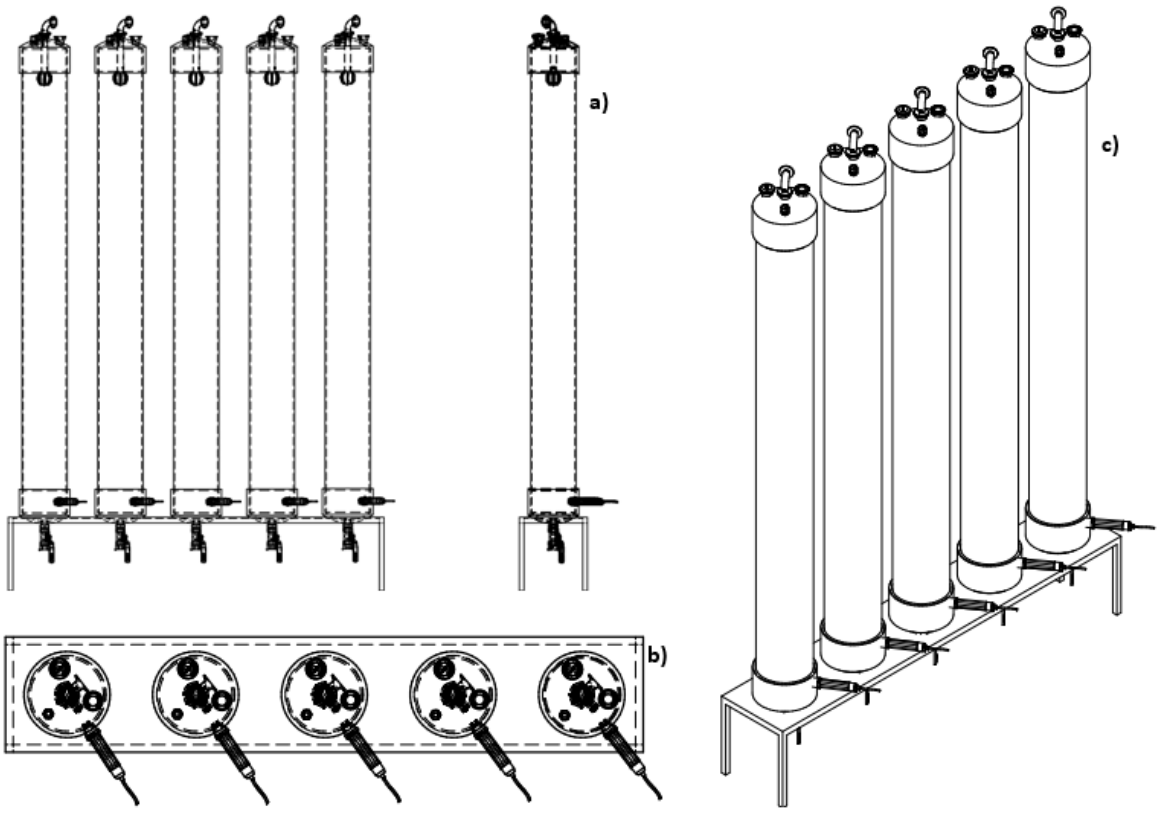

Figure 15: Schematics of the bubble column photobioreactor system, a) front view, b) side view, and c) top view, (Allmicroalgae designs).

2.2.3.5 *CLEANING AND DISINFECTION*

For the cleaning and disinfection of the bubble column photobioreactors, a Cleaning-In-Place (CIP) method was implemented. A pneumatic pump and two hoses were used: one connecting the pump to the spray ball inlet of the reactor and another connecting the pump to the outlet of the reactor (Figure 16) so the water can be recycled from the bottom to the top.

Figure 16: Cleaning system installed, a) overview of the full system, b) hose connected to the top entrance of the bubble column photobioreactor, and c) peristaltic bomb.

After culture harvest, the reactor was filled up with water followed by detergent at 0.63 % (v/v) concentration. Liquid recirculation was possible using a pneumatic pump. After the CIP solution had recirculated 15 to 120 min, the pump was turned off and the water with detergent was discarded. If biofilm remained at the reactor's walls, this step was repeated with the addition of hydrochloric acid (10.5 M) at 0.0083 % (v/v) instead of detergent. After that, the PBR was rinsed three times to remove any residue of the detergent or HCl. The cleaning cycles only stopped when the pH of the rinsing water was lower than 8 and the absorbance at 254 nm was similar to that of demineralized water. This water was then disinfected and used for the next inoculation.

2.2.3.5.1 Total Organic Carbon (TOC)

All the samples taken after each CIP cycle were analyzed to determine the TOC dissolved, and thus infer cleaning efficiency. Each sample was filtered by 0.2 µm filter (Whatman) using a laboratory vacuum pump and had their pH adjusted to 2 with sulfuric acid. Samples were then injected in a TOC-VCSN-Total Organic Carbon analyzer (Shimadzu) with combustion at 720 °C and the method has a measuring range of 0.1 to 4000 mg L^{-1} [47].

2.2.4 COMPARISON OF THREE CULTIVATION SYSTEMS

In this experimental assay, three different cultivation systems were used, namely three 5 L balloon reactors, three 70 L flat panels photobioreactors, and three 60 L bubble column photobioreactors. All replicates started with a biomass concentration of 0.35 g L^{-1}. Culture growing in 5 L balloon reactors was used as inoculum for the three systems. Sampling for optical density analysis was done 3 times a week and sampling for nitrates concentration analysis was done once a week.

The 5 L balloon reactors (Figure 8) were operated as described in Chapter 2.2.1. This assay was followed for 15 days.

The 70 L flat panel photobioreactors (Figure 10) were operated as described in Chapter 2.2.2. This assay was followed for 16 days.

The 60 L bubble column photobioreactors (Figure 17) were kept in constant aeration, and each had one air diffuser. CO_2 was injected by an automatic system to keep pH bellow 8. When pH levels of 8.05 were reached, the CO_2 valve was automatically opened and closed when the pH was 7.95. The temperature was kept between 21 °C and 25 °C. The photobioreactor was kept under constant irradiance (24:0 h photoperiod) of approximately 200 µmol of photons m^{-2} s^{-1}. This trial was followed for 15 days.

Figure 17: Three 60 L bubble column photobioreactors and the light column used.

2.3 GROWTH ASSESSMENT

Optical density was measured at 540, 600, and 750 nm using a spectrophotometer (Genesys 10S UV-VIS). Absorbance values for *Phaeodactylum tricornutum* strain 0018PA and strain 0079PN were measured and dry weight was estimated based on calibration curves, previously determined, represented by equations 2 and 3, respectively.

$$DW = 0.44 \times OD_{600} - 0.04 \quad (2)$$

$$DW = 0.50 \times OD_{600} - 0.03 \quad (3)$$

Biomass concentration was determined by dry weight measurement. This process consisted of the filtration of 10 mL of a culture sample using a 0.7 µm filter and a laboratory vacuum pump. All the filters used were previously weighted. Before the filtration was completed, 10 mL of ammonium formate solution at 35 g L^{-1} was added, as well as demineralized water, in order to wash every salt residue. After complete filtration, the filter was dried at 120 °C and weighted on a DBS 60–30 electronic moisture analyzer (KERN & SOHN GmbH, Balingen, Germany). The dry weight (DW) was calculated by equation 4, where $W\mathrm{a}$ (g) refers to the weight of the filter after the filtration and $W\mathrm{b}$ (g) before, and V (mL) is the filtered volume of the culture sample, which was always 10 mL in this experiment.

$$DW(\mathrm{g\ L^{-1}}) = \frac{W\mathrm{a} - W\mathrm{b}}{V} \quad (4)$$

Volumetric biomass productivity (P) was calculated by equation 5, where X_1 and X_2 correspond to biomass concentration (g L^{-1}) at time t_1 and t_2 (days) of cultivation, respectively.

$$P(\mathrm{g\ L^{-1}\ d^{-1}}) = \frac{X_2 - X_1}{t_2 - t_1} \quad (5)$$

Areal biomass productivity (P_a) was calculated by equation 6, where P is the volumetric biomass productivity (g L^{-1} d^{-1}), V is the volume (L) and A is the implementation area (m^2) of the cultivation system used.

$$P_\mathrm{a}(\mathrm{g\ m^{-2}\ d^{-1}}) = \frac{P \times V}{A} \quad (6)$$

The specific growth rate (µ) was calculated by equation 7, where X_1 and X_2 correspond to biomass concentration (g L^{-1}) at time t_1 and t_2 (days) of cultivation, respectively.

$$\mu(\mathrm{d^{-1}}) = \frac{\ln(X_2) - \ln(X_1)}{t_2 - t_1} \quad (7)$$

2.4 NITRATES DETERMINATION

Nitrate analysis consisted of the centrifugation of 10 mL of culture for 10 min at 3500 rpm, where 250 µL of the supernatant was diluted in 9.45 mL of demineralized water and 300 µL of hydrochloric

acid (1 M). Absorbance was measured at 220 and 275 nm using a spectrophotometer (Genesys 10S UV-VIS) and compared with an in-house sodium nitrate standard calibration curve.

2.5 MICROSCOPY

To evaluate culture contaminants, a Zeiss® Axio Scope A1 coupled with ZEN Axicam 503 (Oberkochen, Germany) colour camera was used, and in to capture and edit the images, the Zen blue 2.5 lite software (ZEISS, Oberkochen, Germany) was used.

2.6 TOTAL VIABLE COUNTS

To determinate the microbial quantity of the cultures, the samples were diluted 1:10 in Ringer solution. This process was repeated sequentially up to 9 times, in order to obtain a count of 30 to 300 CFU (inferior and superior limit).

1 mL of each dilution was put into Petri dishes, and liquid PCA at a temperature of 55 °C was subsequently added. This process is performed in aseptic conditions. Afterwards, the plate is carefully shaken to assure good sample incorporation. After solidification, the plate was incubated in the inverted position for 3 days.

After counting the colonies, results were calculated by equation 8, where N_{colonies} is the colonies count and V (mL) is the volume of sample plated, which was always 1 mL.

$$\text{CFU (Colony} - \text{Forming Unit)/ml} = \frac{N_{\text{colonies}} \times \text{dilution factor}}{V} \quad (8)$$

2.7 BIOCHEMICAL ANALYSIS

2.7.1 PROTEINS

Nitrogen (N) content was estimated at a biomass concentration of 0.1 g L^{-1} by a San++ chemical analyser (SKALAR Breda, the Netherlands) and total protein was estimated by multiplying the N content by a factor of 6.25 [48].

2.7.2 PIGMENTS

In order to extract pigments, 10 mg of fresh biomass was extracted by bead milling with glass beads in 6 mL acetone in the dark. Samples were centrifuged at 3500 rpm for 10 min. This process was repeated until the complete loss of pellet color. The optical density of the supernatant was measured at 380-700 nm with a spectrophotometer (Genesys 10S UV-VIS), obtaining the full absorbance spectrum, that was repeatedly decomposed to the standard pigment spectra. in order to obtain the total pigments content [49].

2.8 STATISTICAL ANALYSIS

The statistical tests were performed using R software (version 4.1.1) through RStudio IDE (version 2021.09.0). The experimental results were analysed considering a 95 % confidence level $(p < 0.05)$. ANOVA was used to compare the data collected, followed by Tukey's multiple comparison tests. The average and standard deviation were calculated, when more than two replicates were available.

3 RESULTS AND DISCUSSION

3.1 *PHAEODACTYLUM TRICORNUTUM* CULTIVATION WATER COMPARISON

At Allmicroalgae, four water types were available for the cultivation of *Phaeodactylum tricornutum*. In order to understand which one would be more suitable, a trial was conducted in twelve 5 L balloon reactors, using municipal, softened, demineralized, and process waters. Growth curves obtained are shown in Figure 18 and global productivities and specific growth achieved are summarized in Table 1.

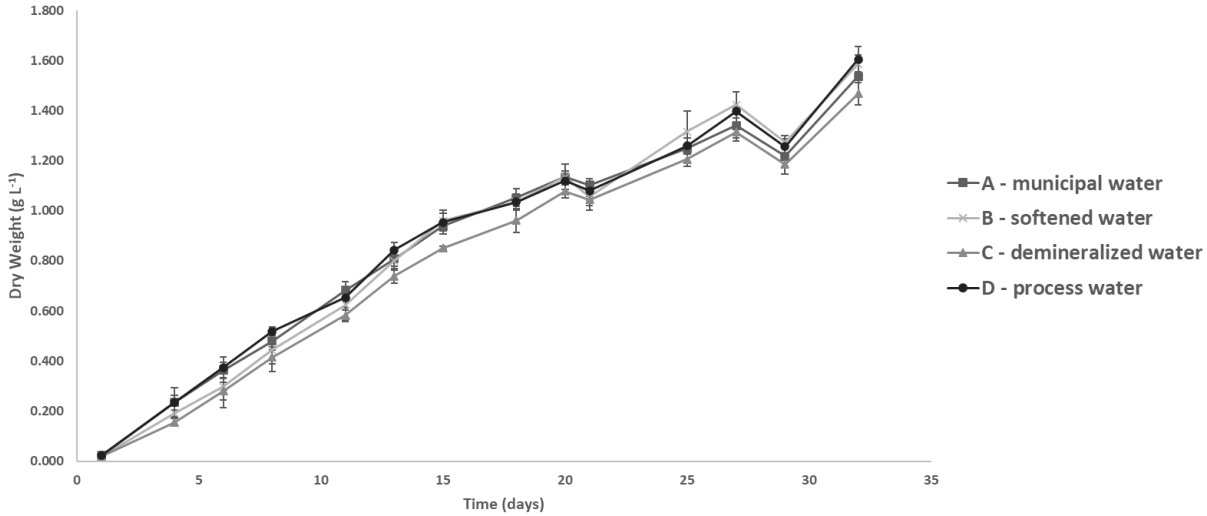

Figure 18: Growth curve of *Phaeodactylum tricornutum* in 5 L balloon reactors, using four different types of water (municipal water, softened water, demineralized water, and process water). The values presented are the average values of the three independent biological replicates and the error bars are the respective standard deviations.

Table 1: Volumetric productivity and specific growth rate of *Phaeodactylum tricornutum*, cultivated in 5 L balloon reactors, using four different types of water (municipal water, softened water, demineralized water, and process water) ($p > 0.05$). The values represent the average and standard deviation of three biologically independent replicates ($n = 3$)

Type of water	Productivity (g L^{-1} d^{-1})	Specific growth rate (d^{-1})
Municipal water	0.047 ± 0.003	0.137 ± 0.005
Softened water	0.049 ± 0.001	0.142 ± 0.001
Demineralized water	0.045 ± 0.001	0.140 ± 0.001
Process water	0.049 ± 0.002	0.139 ± 0.005

The growth parameters showed no statistical differences ($p > 0.05$). Global productivities ranged from 0.045 ± 0.001 g L^{-1} d^{-1} to 0.049 ± 0.002 g L^{-1} d^{-1} and specific growth rates from 0.137 ± 0.005 d^{-1} to 0.140 ± 0.001 d^{-1}. Quelhas, *et al* (2019) obtained global productivities of 0.050 ± 0.003 g L^{-1} d^{-1} to

0.058 ± 0.004 g L^{-1} d^{-1} and specific growth rates of 0.126 ± 0.007 d^{-1} to 0.148 ± 0.012 d^{-1} cultivating *Phaeodactylum tricornutum* in 5 L balloon reactors using ground water, which are according to the results obtained in the present work [22]. Since the productivities and specific growth rates show no statistical differences, it can be concluded that the four different sources of water did not influence the growth of the microalga. Municipal water (local water) was used to successfully cultivate *Phaeodactylum tricornutum* by the team of Conde and Neves on their research work [50]. Therefore, the water used in the subsequent inoculations, municipal water, was strictly chosen by easiest accessibility.

3.2 *PHAEODACTYLUM TRICORNUTUM* STRAINS COMPARISON

Two strains of *Phaeodactylum tricornutum* (0079PN and 0018PA) were cultivated and compared. Since 0018PA was already an in-house known strain, the company previously established the correlation between optical density (600 nm) and DW (Equation 2). However, since strain 0079PN did not have an in-house calibration curve, this correlation was obtained during this work. The calibration curve for the correlation between optical density (600 nm) and DW for the strain 0079PN (Equation 3) is shown in Figure 39, Appendix A.

The first trial was conducted using six 1.5 L balloon reactors. Growth curves are shown in Figure 19, and global productivities and specific growth rates in Table 2.

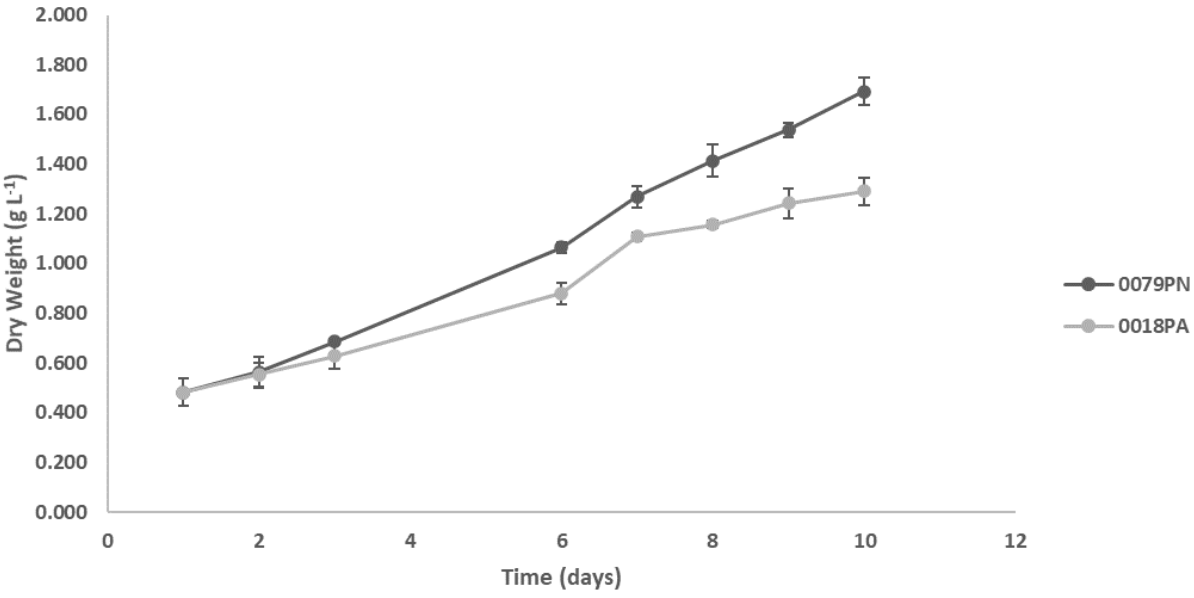

Figure 19: Growth curve of two *Phaeodactylum tricornutum* strains, 0079PN and 0018PA, in 1.5 L balloon reactors. The values presented are the average values of the three independent biological replicates and the error bars are the respective standard deviations.

Table 2: Volumetric productivity and specific growth rate of two *Phaeodactylum tricornutum* strains, 0079PN and 0018PA, cultivated in 1.5 L balloon reactors ($p > 0.05$). The values represent the average and standard deviation of three biologically independent replicates ($n = 3$)

P. tricornutum strain	Productivity (g L^{-1} d^{-1})	Specific growth rate (d^{-1})
0079PN	0.121 ± 0.005	0.139 ± 0.002
0018PA	0.081 ± 0.023	0.110 ± 0.017

Global productivities and specific growth rates of both strains showed no significant differences ($p > 0.05$). 0079PN and 0018PA showed a productivity of 0.121 ± 0.005 g L^{-1} d^{-1} and 0.081 ± 0.023 g L^{-1} d^{-1}, respectively. Quelhas *et al.* (2019) obtained global productivities of 0.050 ± 0.003 g L^{-1} d^{-1} to 0.058 ± 0.004 g L^{-1} d^{-1} and specific growth rates of 0.126 ± 0.007 d^{-1} to 0.148 ± 0.012 d^{-1} when *Phaeodactylum tricornutum* was cultivated in 5 L balloon reactors, which corresponded with the results of this trial, except for 0079PN productivity [22]. However, during comparison of the first 10 days of cultivation to the growth curves of a non-specified strain of *Phaeodactylum tricornutum* obtained by Quelhas *et al.* (2019), concentration of the strain 0079PN obtained in this trial was higher which subsequently led to higher productivity [22].

To validate the obtained results at a higher scale, a second trial was conducted in six 70 L flat panel photobioreactors. This trial was also done to explore if there were any differences between the strains regarding their resistance to summer temperatures, in order to be able to have higher temperature flexibility when cultivating in the bubble column photobioreactor. However, the irrigation system was not activated during the 2nd and 3rd cultivation day, during which the temperatures in Pataias, Leiria were elevated (29 °C and 30 °C, respectively) [51]. Therefore, the cultures did not survive (Figure 20). The temperature of the culture is usually higher than the ambient temperature [42], and according to Siqueira *et al.* (1993), *Phaeodactylum tricornutum* was unable to survive 31°C [52].

Figure 20: *Phaeodactylum tricornutum* cultivated in 70 L flat panels photobioreactor presenting a yellow color, which indicated death.

Once the weather conditions felt at that time of the year in Pataias did not allow the outdoor cultivation of *P. tricornutum*, the Algem® lab-scale photobioreactor was used to validate the results obtained in the culture room. This PBR is able to model monthly light and temperature profiles of a specific place and at a particular time of the year [53]. Therefore, the Algem® was used to understand how both strains would behave during summer and winter in Pataias, Leiria. Both strains' summer and winter growth curves obtained on the Algem® software are shown in Figure 21 and Figure 22, respectively. Global productivities and specific growth rates, obtained with the concentrations measured before starting the Algem® lab-scale PBR and after it ended, are shown in (Table 3).

In the Algem® lab-scale photobioreactor, 0079PN global productivity and specific growth rate of 0.150 g L^{-1} d^{-1} and 0.213 d^{-1}, respectively. During winter, 0018PA showed the highest global productivity and specific growth rate of 0.050 g L^{-1} d^{-1} and 0.204 d^{-1}. Both strains presented higher productivities and SGR during summer. This was expected since during winter the biomass productivity is limited by low light availability [54].

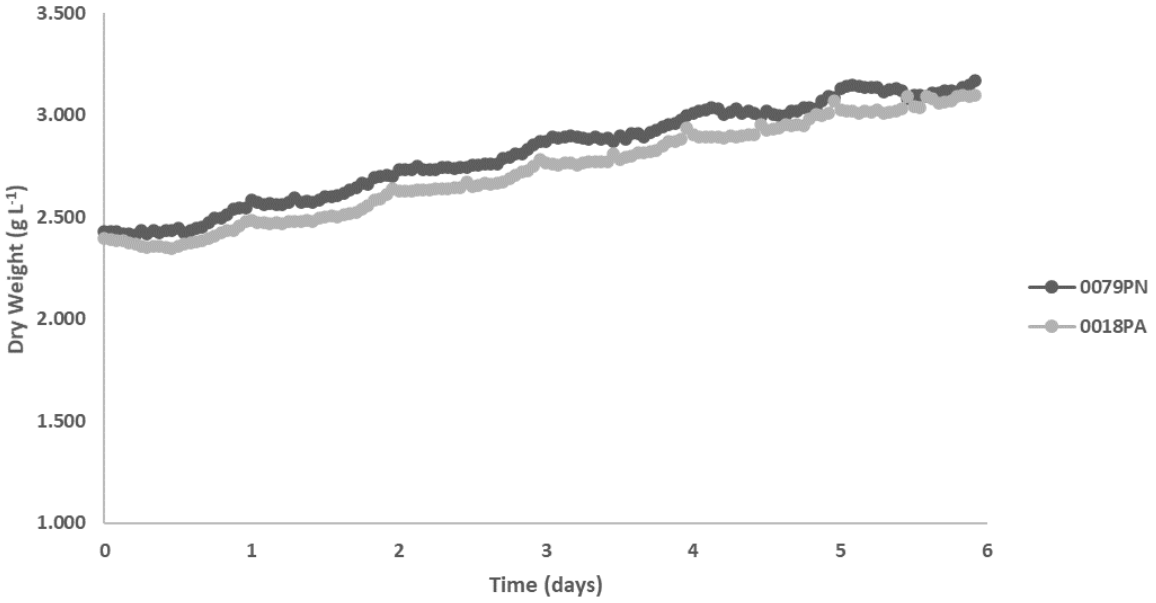

Figure 21: Growth curve of two strains of *Phaeodactylum tricornutum*, 0079PN and 0018PA, cultivated in the Algem® lab-scale photobioreactor, during summer (n = 1).

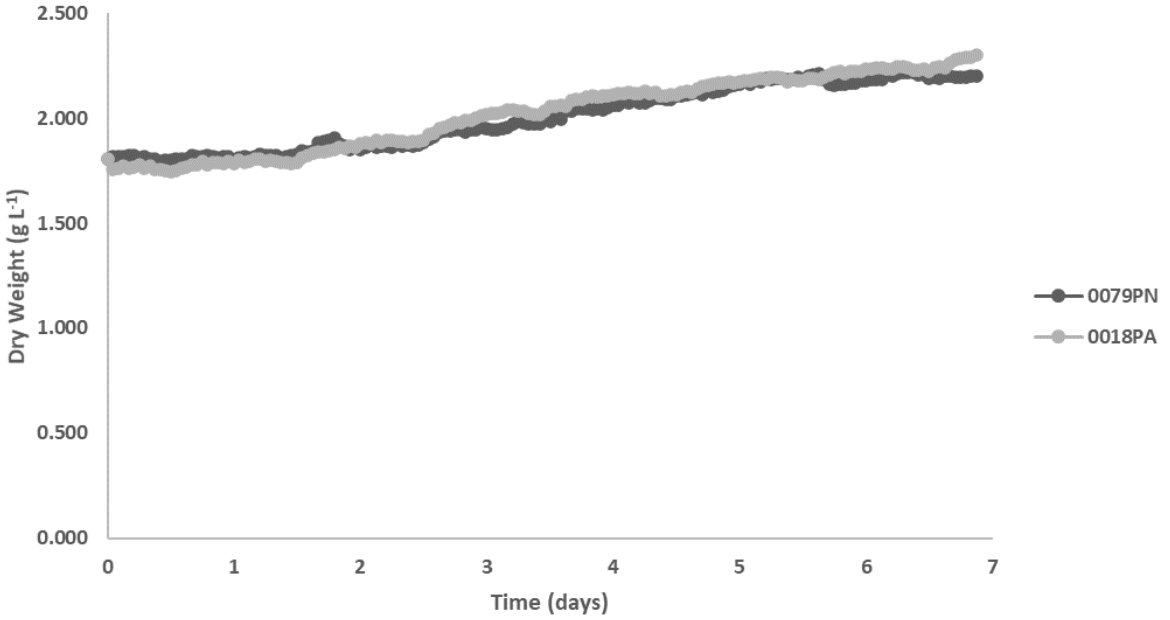

Figure 22: Growth curve of two strains of *Phaeodactylum tricornutum*, 0079PN and 0018PA, cultivated in the Algem® lab-scale photobioreactor, during winter (n = 1).

Table 3: Global volumetric productivity and specific growth rate of two strains of *Phaeodactylum tricornutum*, 0079PN and 0018PA, cultivated in the Algem® lab-scale photobioreactor, during summer and winter (n = 1)

Season	*P. tricornutum* strain	Productivity (g L^{-1} d^{-1})	Specific growth rate (d^{-1})
Summer	0079PN	0.150	0.213
	0018PA	0.131	0.198
Winter	0079PN	0.033	0.116
	0018PA	0.050	0.204

Based on the 1.5 L balloon reactors trial, the two strains present no statistically significant differences, and based on the Algem® lab-scale photobioreactor trial, one strain presented the highest values in one season and the other strain in the other season. Therefore, since the company had already been cultivating the strain 0018PA at the industrial scale, this strain was chosen for following trials due to more knowledge about it, easier accessibility, and more inoculum availability.

3.3 BUBBLE COLUMN PHOTOBIOREACTOR OPTIMIZATION

3.3.1 AIR DIFFUSER AND pH CONTROLLER

Many factors influence microalgae growth, one of them being the pH of the culture medium leading to productivity decrease/increase [15–17]. Therefore, it was essential to have this parameter regulated and optimized. Sufficient mixing provides a better homogenization of the culture, allowing movement of the cells, and reducing the shading effect [37]. Furthermore, adequate mixing can prevent sedimentation when the culture concentration is high [15]. These parameters needed to be taken into consideration. Several experiments were conducted using bubble column photobioreactors and the first set of experiments included mixing and homogenization, and optimization of pH regulation. Global and maximum productivities and specific growth rates were calculated and are shown in Table 4.

During the first inoculation, it was clear that a single sparger was not able to provide sufficient mixing to the whole reactor, as it is visible in Figure 23 a). The addition of another sparger resulted in better mixing and a more homogenized culture (Figure 23 b.1) and b.2)). This second sparger had a ring shape (with a diameter of approximately 12 cm) that provided more bubbles in the bottom of the reactor, especially closer to the walls. The first sparger supplemented more bubbles in the middle to top.

Furthermore, an automated pH control system was added, set at pH 8, providing easier management of the reactor. Thereby, the pH of the second trial was kept stable, ranging from 7.89 to 8.38, contrary to the first trial, which varied from 6.26 to 9.27, (Figure 24). Consequently, sampling for pH analysis was not as frequent anymore and pH regularization was achieved.

Figure 23: Bubble column photobioreactor mixing provided by a) one sparger and b.1) and b.2) with two spargers.

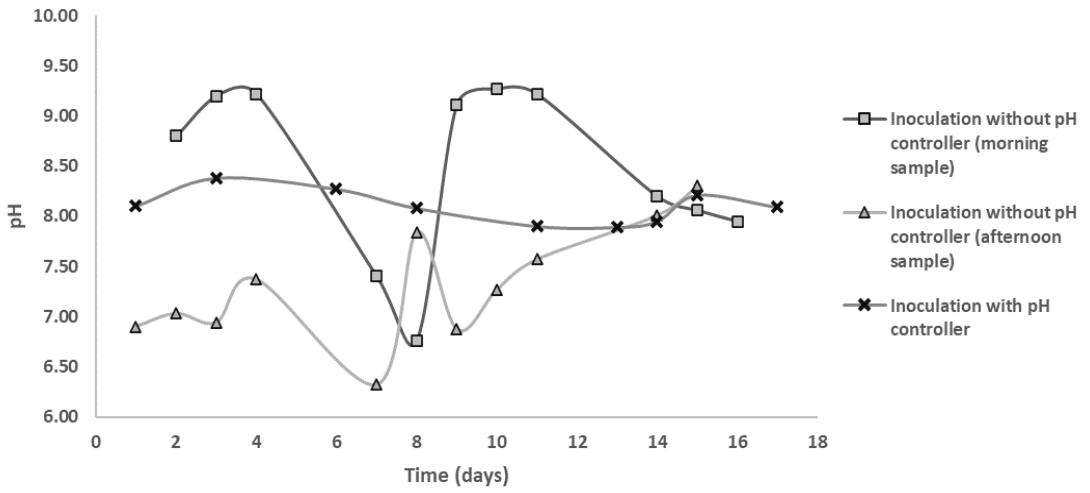

Figure 24: pH of a *Phaeodactylum tricornutum* culture growing in two different 60 L bubble column photobioreactors (with and without a pH controller). Sampling on the PBR without pH controller was done twice per day (morning and afternoon).

Table 4: Global and maximum volumetric productivities and specific growth rates of *Phaeodactylum tricornutum*, cultivated in 60 L bubble column photobioreactor, before and after changes. The values for the last represent the average and standard deviation of two biologically independent replicates

Inoculation	Productivity (g L^{-1} d^{-1})		Specific growth rate (d^{-1})	
	Global	Maximum	Global	Maximum
Before changes (n = 1)	0.06	0.11	0.16	0.33
After changes (n = 2)	0.07 ± 0.00	0.13 ± 0.01	0.14 ± 0.01	0.34 ± 0.04

All parameters shown in Table 4 were higher in the improved design of the bubble column photobioreactor, except for the global specific growth rate. These improvements led to a 11 %, 18 %, and 5 % increase in global and maximum productivity, and maximum SGR. On the other hand, it showed a 12 % decrease in global SGR. However, replicates would be necessary for a statistical evaluation and definitive conclusions. Branco-Vieira *et al.* (2018) obtained a maximum volumetric productivity of 0.13 g L^{-1} d^{-1} and a maximum specific growth rate of 0.17 d^{-1} while cultivating *Phaeodactylum tricornutum* in an outdoor 800 L bubble column PBR [55]. This did not correspond to the productivity obtained from the inoculation before changes, nor to the reached maximum specific growth rates. However, the volumes of the bubble columns used were very different (as opposed to 60 L bubble column used in this work). This project's higher maximum specific growth rates might have been due to 24h:0 photoperiod. On the other hand, not presenting an efficient mixing and a stabilized pH might have caused the lower maximum productivity of the inoculation before changes when compared to the 800 L PBR.

Mixing and homogenization were improved after alteration was applied to the reactor. Labor work was reduced as a consequence of pH stabilization.

3.3.2 LIGHT SYSTEM

Since the availability and intensity of light is one of the main parameters to consider in algae cultivation [16, 18], there was a need to optimize it. Three different light systems installed in the bubble column photobioreactors (Figure 25) were tested.

Figure 25: Bubble column photobioreactors, a) with a back and front metal sheet yellow light system, b) with a back and front metal sheet white light system, and c) with a front metal sheet yellow light system.

The installation of the light system (Figure 25 c)), which was kept 17.2 cm of the edge of the bioreactor, under 760 µmol of photons m^{-2} s^{-1}, resulted in a green color culture with green foam (Figure 26), which indicated cell death. This was caused by the high temperature that the culture reached, since temperatures above optimal or sudden changes in temperature lead to the decline of algal growth, or even death of algae cells [17, 18].

To understand the temperatures reached by the culture due to the light system's distance, the maximum temperatures inside the reactor were measured while keeping the lights at five different distances (7.5 cm, 11.7 cm, 17.2 cm, 24.0 cm, 27.1 cm). During the trials, the light system was kept on stage 36 (as mentioned above, maximum intensity reached by the light system). The results are shown in Figure 27.

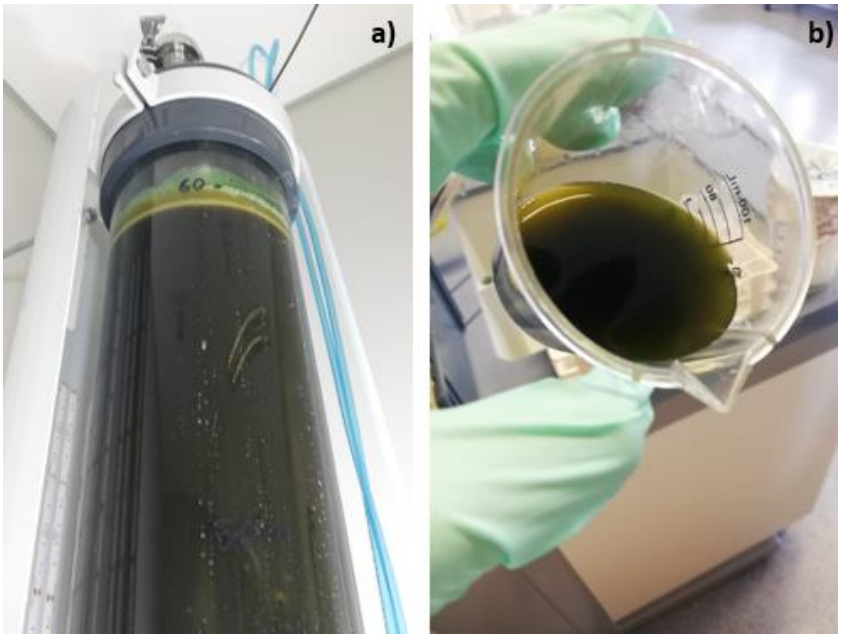

Figure 26: *Phaeodactylum tricornutum* cultivated in 60 L bubble column photobioreactor presented a green color, which indicated death.

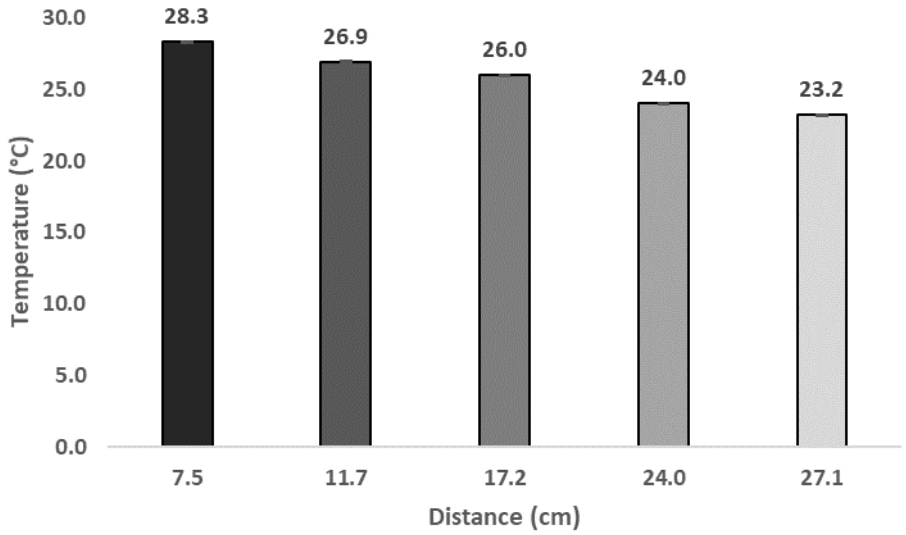

Figure 27: Maximum temperature reached inside the bubble column photobioreactor at different distances from the reactor to the back metal sheet yellow light system.

The temperature reached at the 17.2 cm distance was 26.0 ± 0.1 °C. However, as microalgae absorb light, tubular photobioreactors tend to overheat, and the temperature of the culture was higher (> 35 °C), which caused cell death [34, 56].

The distance of 27.1 cm resulted in the lowest temperature; hence it was chosen for the following inoculations. Furthermore, a wider distance allowed the possibility of adding a ventilator, favoring better air circulation.

The photon flux density (µmol m^{-2} s^{-1}) of the light was measured at different distances from the lights to the reactor. Figure 28 shows the results for the chosen distance (27.1 cm) in 4 chosen stages of light intensity, namely: 9, 18, 27, and 36, which correspond to 25 %, 50 %, 75 %, and 100 % of the total system capacity, respectively, at different points of the reactor.

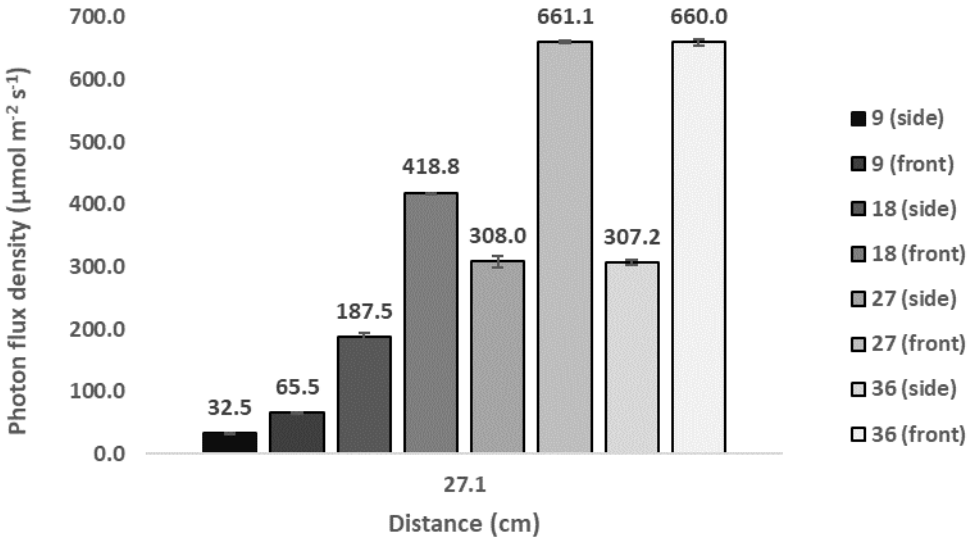

Figure 28: Photon flux density in different stages of light intensity and two different points of the bubble column photobioreactor, front and side. The values presented are the average values of the three independent replicates and the error bars are the respective standard deviations.

As previously said, the optimal light intensity is generally 200 to 400 µmol m^{-2} s^{-1} for most microalgae species [15]. Nur *et al.* (2019) obtained the highest growth rates for *Phaeodactylum tricornutum* cultivation under 300 µmol m^{-2} s^{-1} [57]. However, 300 µmol m^{-2} s^{-1} was not obtained in any of the stages tested. According to Lambert-Beer's law (Equation 1), the light that penetrates the culture gets attenuated by it [15]. Consequently, stage 9 (32.5 – 65.5 µmol m^{-2} s^{-1}) would not have sufficient photon flux density to cultivate *Phaeodactylum tricornutum*, and stage 18 (187.5 – 418.8 µmol m^{-2} s^{-1}) therefore seemed like the most suitable for this microalga cultivation. The light system was decided to be kept at 27.1 cm from the reactor and on stage 18 for the rest of the trials.

After the conditions of the light system were settled, the three different light systems were tested and compared. Results for global and maximum productivities are shown in Figure 29 and results for global and maximum specific growth rates are shown in Figure 30.

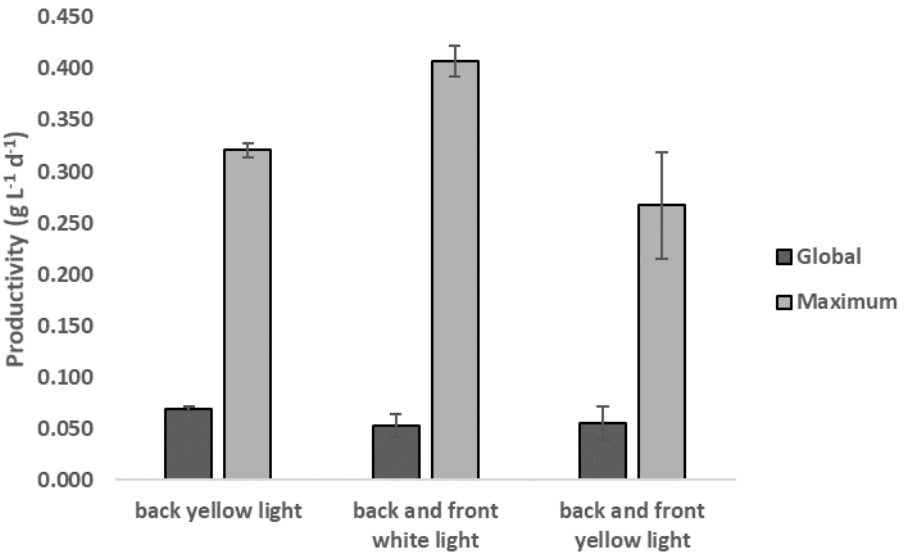

Figure 29: Global and maximum volumetric productivity of *Phaeodactylum tricornutum*, cultivated in 60 L bubble column photobioreactors using three different light systems. The values presented are the average values of the two independent biological replicates and the error bars are the respective standard deviations.

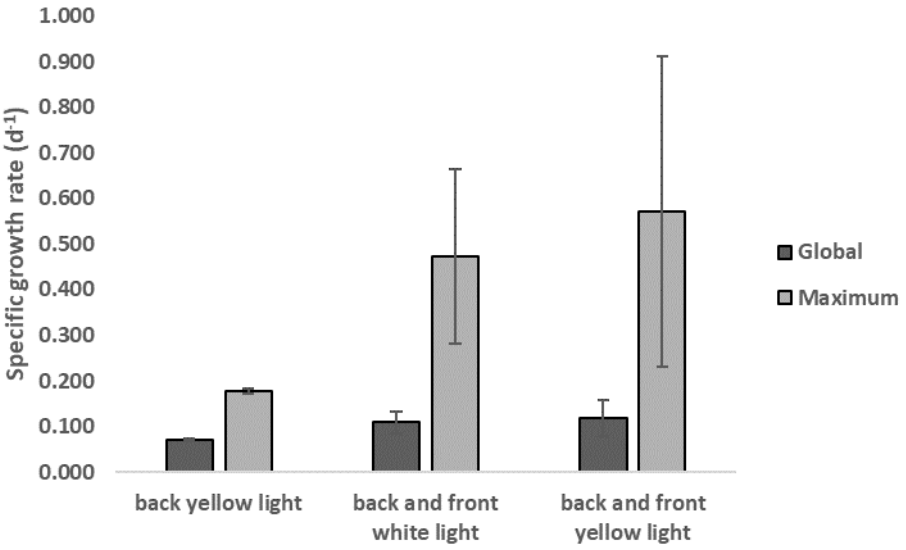

Figure 30: Global and maximum specific growth rate of *Phaeodactylum tricornutum*, cultivated in 60 L bubble column photobioreactors using three different light systems. The values presented are the average values of the two independent biological replicates and the error bars are the respective standard deviations.

The light system installed in the back of the photobioreactor with yellow LED lights presented the highest global productivity of 0.07 ± 0.00 g L^{-1} d^{-1}. The highest maximum productivity, of 0.41 ± 0.02 g L^{-1} d^{-1}, was reached on the bioreactor with the light system installed on both sides with white light. On the other hand, the yellow light installed in the back and the front of the photobioreactor resulted in the highest *P. tricornutum* global and maximum specific growth rate: 0.12 ± 0.04 d^{-1} and 0.57 ± 0.34 d^{-1},

respectively. However, no statistical conclusions were made due to the absence of triplicates. More trials needed to be conducted under these conditions to compare them. Branco-Vieira *et al.* (2018) obtained a maximum volumetric productivity of 0.13 g L^{-1} d^{-1} and a maximum specific growth rate of 0.17 d^{-1} cultivating *Phaeodactylum tricornutum* in an outdoor 800 L bubble column PBR [55]. This did not correspond to the values obtained except for the lowest maximum specific growth rate obtained in the back yellow light system. However, the volumes of the bubble columns used were very different and the bubble column used by Branco-Vieira's team was under natural conditions. The 24h:0 photoperiod the bubble columns in this project were under during the whole cultivation might have caused higher values. The smaller volume, as well as smaller diameter, of the bubble column in this project (0.19 cm in this project compared to 0.45 cm in the 800 L bubble columns), might have led to less shading effect. Moreover, in indoor reactors, the temperature can be controlled.

Furthermore, the growth parameters obtained with the three different light systems were compared to the previous bubble column version (condition of 2 spargers, with a pH controller, no light system): the back yellow light presented an increase of 1 % and 155 % in global and maximum productivity, respectively, and a decrease of 50 % and 48 % in global and maximum SGR, respectively; the back and front white light presented an increase of 223 % and 39 % in maximum productivity and SGR, respectively, and a decrease of 22 % and 24 % in global productivity and SGR, respectively; and the back and front yellow light presented an increase of 64 % and 68 % in maximum productivity and SGR, respectively, and a decrease of 19 % and 18 % in global productivity and SGR, respectively. However, regarding the maximum specific growth rates of the light systems in the back and front of the reactor, the associated error was too high, making this parameter non credible for comparison.

3.3.2.1 BIOCHEMICAL CHARACTERIZATION OF THE BIOMASS

At the end of the trials, *P. tricornutum* biomass was collected, and biochemical analysis was performed. Results are shown in Table 5.

Table 5: *Phaeodactylum tricornutum* protein and pigments contents, cultivated in 60 L bubble column photobioreactors using three light systems. The values represent the average and standard deviation of two biologically independent replicates (n = 2)

Light system	Protein (%)	Total Carotenoids (mg g^{-1} *DW*)
Back yellow light	41.84 ± 3.93	10.91 ± 0.35
Back and front white light	52.06 ± 3.73	12.79 ± 0.15
Back and front yellow light	54.90 ± 3.85	11.73 ± 0.19

The highest protein content, 54.90 ± 3.85 %, was achieved using the yellow LED system from both sides. However, small difference was found between the protein content of this light system and the same when illuminating only on one side. Back yellow LED-illuminated cultures presented the lowest protein content. Quelhas *et al.* (2017) obtained protein levels of *Phaeodactylum tricornutum* of 51.2 % up to 54.7 % [22], which was according to the content obtained using both light systems in the back and the front of the bubble column PBRs. However, the back yellow light system did not reach these protein levels. These differences might have been due to different cultivation systems, since the research was done in 5 L balloon reactors and not in 60 L bubble column photobioreactors, like in this project. Furthermore, back and front yellow light systems presented 24 % and 5 % higher content over the back yellow light, and back and front white light, respectively.

The system with white LEDs featured the highest total carotenoid content, 12.79 ± 0.15 mg g^{-1} *DW*. Furthermore, it presented 15 % and 8 % higher total carotenoid content when compared to back yellow light and back and front yellow light, respectively. However, the difference of total carotenoids between the three light systems was low. Di Lena *et al.* (2018) obtained total carotenoids levels of *Phaeodactylum tricornutum* of 10,22 mg g^{-1} *DW* [58]. All values obtained are similar to the literature.

In conclusion, both back and front light systems presented an overall improvement – growth parameters, protein, and total carotenoids – over the back yellow light system.

3.3.3 OPERATION IN SEMI-CONTINUOUS REGIME

The Ruiz model can predict biomass production and maximum productivity in continuous operation regimes, from kinetic growth parameters obtained from a batch experiment [46].

A batch cycle was conducted in three bubble column PBRs. The Ruiz model was used to understand the conditions required to operate this system in a continuous regime and predict biomass productivity. *Phaeodactylum tricornutum* biomass evolution during and after the non-linear regression of the batch cycle done by the model is shown in Figure 31. Furthermore, the data collected from the batch cycle was adjusted using Excel add-in Solver and results in the growth kinetic parameters are shown in Table 6.

When the volume of the reactor (60 L) was divided by the hydraulic retention time (10 days), a flow rate of 6 L d^{-1} was obtained. This meant that 6 L of culture needed to be harvested and renovated every day in order to operate this system in a continuous regime.

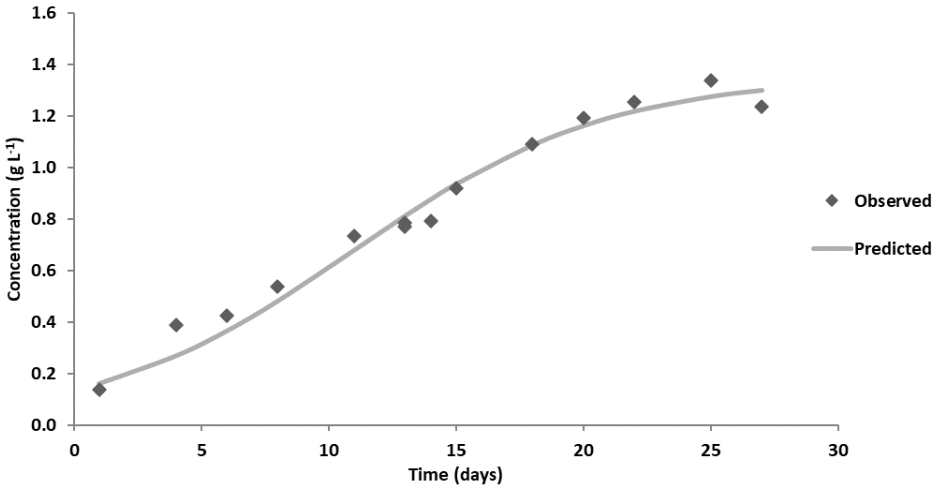

Figure 31: Biomass evolution of *Phaeodactylum Tricornutum* during a batch cycle. Symbols are experimental data and solid lines depict the predicted data.

Table 6: Kinetic growth parameters obtained by the Ruiz model

Parameters	
Specific growth rate, μ (d^{-1})	0.20
Batch maximum productivity (g L^{-1} d^{-1})	0.06
Continuous productivity (g L^{-1} d^{-1})	0.07
Correlation coefficient, *R*	0.97
HRT (days)	10

In order to keep an operational continuous regime based on collected data, the culture needed to be maintained in a constant concentration of approximately 0.8 g L^{-1}, which is when maximum productivity would be reached. Culture and medium needed to be introduced in the reactor with the same flowrate (6 L d^{-1}) that the culture would be harvested. Furthermore, the biomass concentration in the harvested culture would have to be equal to the biomass concentration in the reactor [46].

However, the continuous regime was not possible to be operated due to absence of equipment. A possible way to operate in this regime, would have been if each bubble column featured two hoses/tubes, a peristaltic pump (with the correct flowrate settled), and two storage tanks (one for water and medium and another for the harvested culture). Furthermore, only two tanks with sufficient volume storage would have been needed for the whole bubble column systems. Labor work would only be required to refill and harvest the storage tanks.

Instead, a semi-continuous regime was tested in the bubble column systems. This system was operated with renovation once every three days. Since the renovation volume for a continuous regime

given by the Ruiz model was 6 L per day, the renovation volume for the semi-continuous regime was adjusted to 3 days and 18 L.

The exponential phase of the batch cycle was from the 8th (concentration of 0.5 g L^{-1}) to the 15th (0.9 g L^{-1}) day of cultivation (Figure 31). From the 11th (0.7 g L^{-1}) to the 14th (0.9 g L^{-1}) day of cultivation, the highest productivities were reached. Consequently, it was settled that the semi-continuous regime would start with a concentration of approximately 0.7 g L^{-1}. The growth curve obtained with this semi-continuous regime is shown in Figure 32.

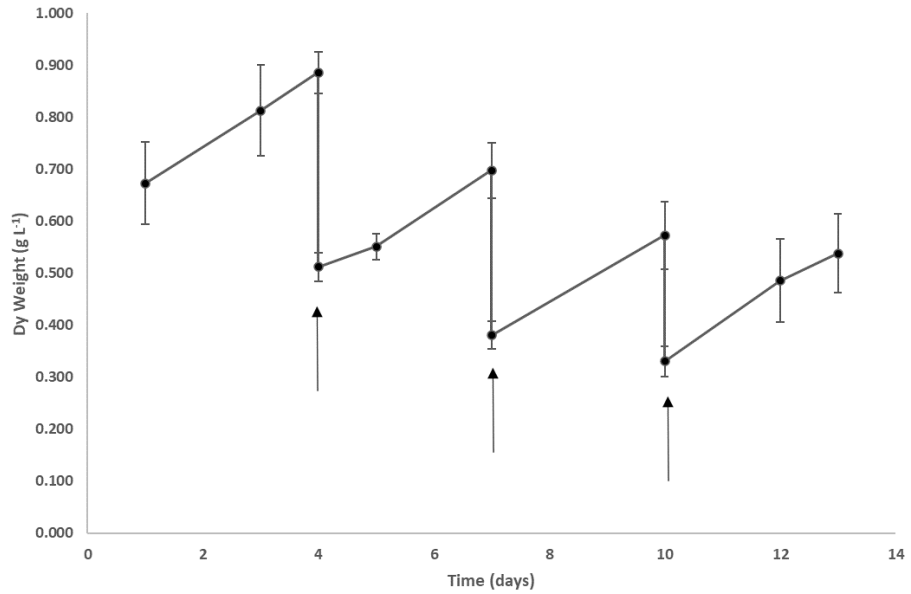

Figure 32: Growth curve of *Phaeodactylum tricornutum*, cultivated in 60 L bubble column photobioreactors, in a semi-continuous operation regime, with a once in 3 days renovation. The arrows represent each renovation. The values presented are the average values of the three independent biological replicates and the error bars are the respective standard deviations.

Productivities and specific growth rates obtained in each renovation presented no statistically significant differences ($p > 0.05$). However, the starting concentration of each renovation was lower than the previous. Due to the high dilution rate, washout occurred and consequently, after 3 days, the biomass did not reach 0.9 g L^{-1}. In conclusion, this semi-continuous operation was not successful.

In order to have obtained a successful semi-continuous operation regime, all cycles after renovation should have started at concentration of approximately 0.7 g L^{-1}, and after 3 days, a concentration of 0.9 g L^{-1} would have been reached according to the obtained data. If this concentration was not reached, either time (waiting until 0.9 g L^{-1} was reached) or volume (less renovation volume due to lower reached concentration) should have been adjusted.

Lastly, a 38 % and a 67 %, increase in biomass production would be reached if the bubble column system was operated under a successful semi-continuous and continuous regime, respectively, with the expected results mentioned above. Furthermore, this increase would have been 60 % and 67 %, respectively, in volumetric productivity. When compared to the batch cycle, Guerra *et al.* (2021) obtained a 1.5-fold increase in biomass volumetric productivity during a semi-continuous and a continuous regime [59].

3.3.4 CLEANING AND DISINFECTION

Achieving a good cleaning and sterilization was an important parameter. These PBRs have a high probability of biofilm formation and uncontrolled growth of pathogenic microorganisms in its inner walls [15]. In order to start a new cycle, the reactor needed to be disinfected. A thorough cleaning is essential for an optimal growth performance and even more so when the final product is for human consumption.

To evaluate the cleaning and sterilization of the bubble column photobioreactor, three cleaning trials were done. For an efficient cleaning, the final pH must be < 8, and the 254 nm absorbance must be close to 0.000 (demineralized water). These values were always reached on the 3rd water renovation. Absorbance 254 nm and Total Organic Carbon (TOC) of the cleaning trial (using just detergent) are shown in Figure 34 and Figure 35, respectively.

However, using just the detergent during one cycle let to a not proper cleaning, which was done twice and was still ineffective (Figure 33 c)). Consequently, there was a need to introduce an acid wash with HCl (Figure 33 d)). This cleaning is recommended when there is high biofilm formation, attaching to the reactor walls. 254 nm optical density and Total Organic Carbon (TOC) measured are shown in Figure 36 and Figure 37, respectively.

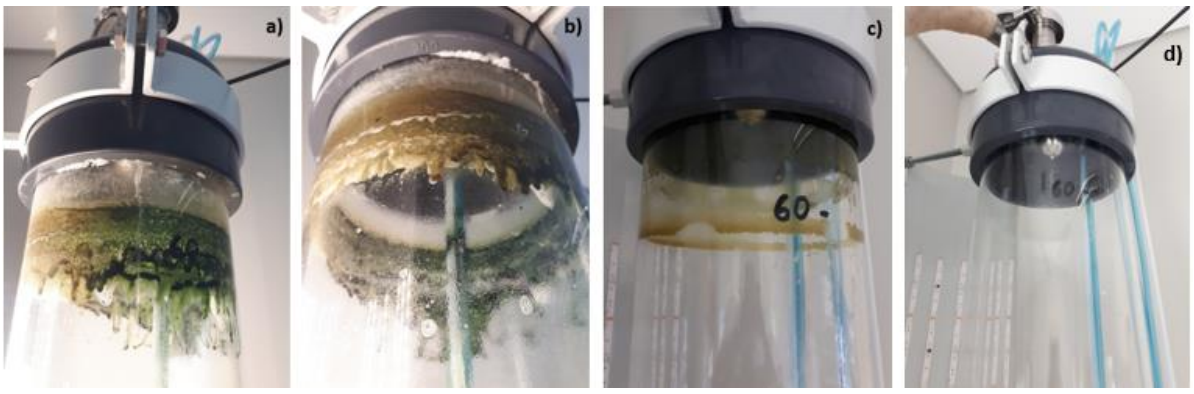

Figure 33: Bubble column photobioreactor after total culture harvesting, a) and b) before any cleaning stage, c) after using detergent twice, and d) after using HCl.

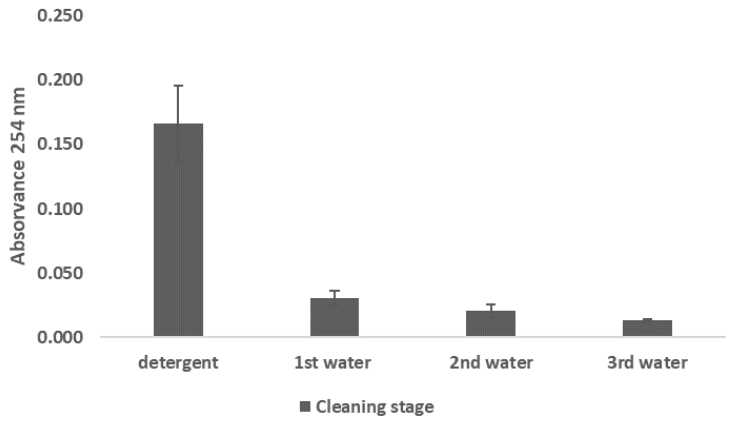

Figure 34: Absorbance 254 nm of samples taken after every cleaning stage of a bubble column photobioreactor. The values presented are the average values of the four independent replicates and the error bars are the respective standard deviations.

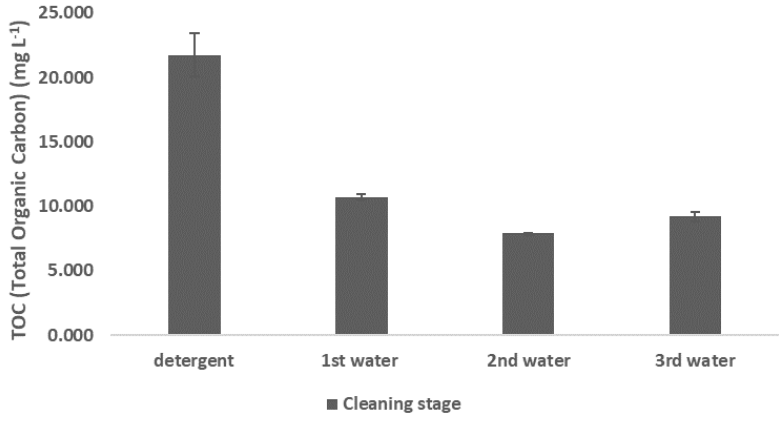

Figure 35: Total organic carbon of samples taken after every cleaning stage of a bubble column photobioreactor. The values presented are the average values of the two independent replicates and the error bars are the respective standard deviations.

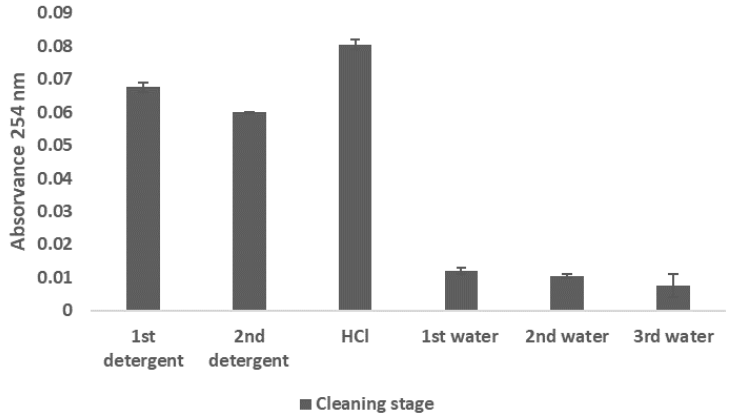

Figure 36: Absorbance 254 nm of samples taken after every cleaning stage of a bubble column photobioreactor (trial with HCl). The values presented are the average values of the two independent replicates and the error bars are the respective standard deviations.

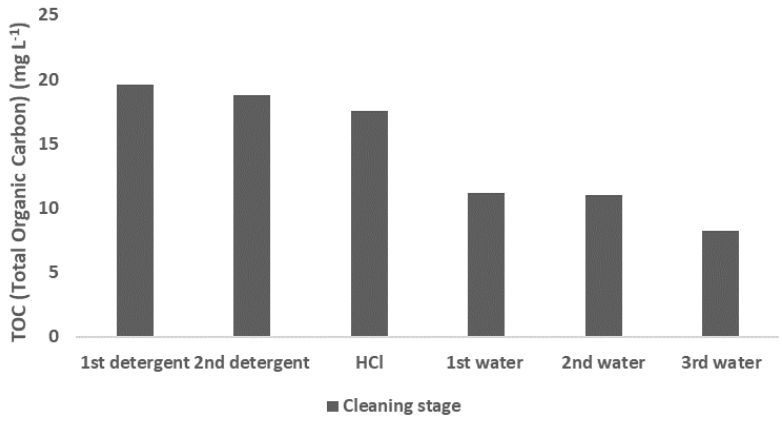

Figure 37: Total organic carbon of samples taken after every cleaning stage of a bubble column photobioreactor (trial with HCl) (n = 1).

During the cleaning of the reactor, in both cases, both absorbance (254 nm) and TOC decreased alongside with cleaning stages.

3.4 COMPARISON OF THREE CULTIVATION SYSTEMS

Another goal of this project was to optimize the scale-up process in the company. In order to understand better if the addition of a bubble column PBR system would optimize the process, this system was compared with other two systems, a 5 L balloon reactor system and a 70 L flat panel PBR system.

3.4.1 GROWTH ASSESSMENT

Parameters related to microalgae growth, such as productivity and specific growth rate were first compared. The growth curves of this trial are shown in Figure 38. Global and maximum productivities, and global and maximum specific growth rates for each system are shown in Table 7.

The bubble column showed the highest global and maximum areal productivity and maximum volumetric productivity, with statistical differences ($p < 0.05$). The results of areal productivity were expected due to bubble column and flat panel's higher volume than balloon reactors, while all three had a similar surface area. Furthermore, the bubble column presented higher productivity than flat panels. Unlike the flat panels, this might have been caused by the 24h:0 photoperiod in the bubble columns, and better pH regularization achieved by the automated pH controller that the flat panel did not include. The balloon reactor achieved the highest global volumetric productivity, with statistical differences ($p < 0.05$). This might have been due to optimal conditions being easier to reach on a small scale, providing better conditions for microalgae to grow [28]. The growth parameters obtained using 5 L balloons in this project were similar to those achieved by Quelhas *et al.* (2019) [22]. However, values obtained on the flat panels did not agree with Maia *et al.* (2021) [60]. A possible reason could have been the pH

regularization. In this case, the CO_2 valve needed to be manually opened, which is not a precise regulation. As most species are sensitive to pH values above and below their optimal range, this can lead to productivity decrease [15–17]. Compared to Branco-Vieira *et al.* (2018), growth parameters achieved in the 800 L bubble column were equal to values laid out in Table 7 [55].

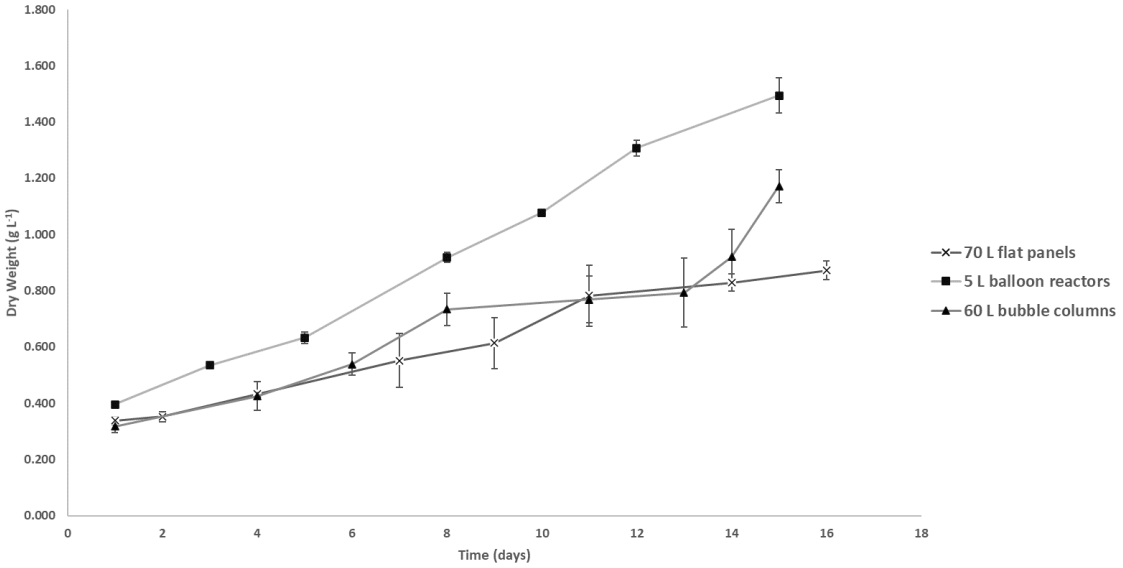

Figure 38: Growth curve of *Phaeodactylum tricornutum*, cultivated in three different systems. The values presented are the average values of the three independent biological replicates, and the error bars are the respective standard deviations.

Table 7: Global and maximum volumetric productivity, areal productivity, and specific growth rate of *Phaeodactylum tricornutum*, cultivated in three different systems. The values represent the average and standard deviation of three biologically independent replicates ($n = 3$). Different small letters in the same column indicate significant differences at $p < 0.05$

Photobioreactor	Productivity (g L^{-1} d^{-1})		Areal Productivity (g m^{-2} d^{-1})		Specific growth rate (d^{-1})	
	Global	Maximum	Global	Maximum	Global	Maximum
5 L balloon reactor	0.07 ± 0.00 a	0.12 ± 0.01 a	4.07 ± 0.23 a	6.42 ± 0.77 a	0.09 ± 0.00 a	0.15 ± 0.01 a
70 L flat panel	0.03 ± 0.000 b	0.09 ± 0.02 a	22.07 ± 1.53 b	61.41 ± 12.81 a	0.06 ± 0.00 b	0.14 ± 0.02 a
60 L bubble column	0.06 ± 0.00 c	0.25 ± 0.08 b	33.34 ± 2.27 c	147.33 ± 43.99 b	0.09 ± 0.01 a	0.26 ± 0.07 a

3.4.2 BIOCHEMICAL CHARACTERIZATION OF THE BIOMASS

In order to understand the differences in the biochemical composition of *Phaeodactylum tricornutum* cultivated in three different systems, protein level and total carotenoid yield were analysed on the resultant biomass. Results are shown in Table 8.

Table 8: *Phaeodactylum tricornutum* protein and total carotenoid contents, cultivated in three different systems. The values represent the average and standard deviation of three biologically independent replicates ($n = 3$). Different small letters in the same column indicate significant differences at $p < 0.05$

Photobioreactor	Protein (%)	Total Carotenoids (mg g^{-1} *DW*)
5 L balloon reactor	60.54 ± 2.97 a	21.24 ± 0.69 a
70 L flat panel	33.39 ± 1.96 b	9.15 ± 0.54 b
60 L bubble column	39.37 ± 9.21 b	16.05 ± 3.86 a

Protein levels were statistically higher in biomass obtained grown in 5 L balloons, and total carotenoids were statistically lower in 70 L flat panel. Protein and pigment composition can be influenced by light availability [42, 49], noticed in the flat panel biomass. Quelhas *et al.* (2017) obtained 51.2 % up to 54.7 % *P. tricornutum* protein levels in their work [22], which was lower than the ones obtained in this project in 5 L, and higher than those in the other two systems. Di Lena *et al.* (2018) obtained total carotenoids levels of *Phaeodactylum tricornutum* of 10,22 mg g^{-1} *DW* [58], which are similar or lower than the ones obtained in this work.

3.4.3 TOTAL VIABLE COUNT EVOLUTION

Total viable count (TVC) is a test that can estimate the total number of microorganisms, such as bacteria, yeast, or mold species, presented in a sample. This test provides an overall indication of the quality of the culture. This is very important since products intended for pharmaceutical and functional food sectors must be free of bacterial contamination [11].

Each system was sampled in the first and last days of cultivation and results are summarized in Table 9.

All results are similar between each other ($p > 0.05$). Furthermore, it is notable that the total viable count increased when the culture was added to the medium and after the cultivation cycle. The sample labeled as 'before inoculation' was taken after the neutralization of the cultivation water mixed with the medium. Both flat panels and bubble columns were inoculated using 5 L balloon reactors. However, these inoculations were not done under sterile conditions, which increased the microbial load

in these systems. Furthermore, from the beginning of the cycle until its end, the microbial load increased approximately by 10 %, 17 %, and 19 % in balloons, flat panels, and bubble columns, respectively. Microorganisms can also grow during cultivation due to nutrient supplementation, leading to an increase in TVC. However, it was expected that balloon reactors would have the lowest values since all procedures were done under sterile conditions.

Table 9: Total viable counts obtained in three different systems, before and after inoculation, and at the end of the cultivation cycle ($p > 0.05$)

Photobioreactor	TVC - Total Viable Counts (log CFU mL^{-1})		
	Before inoculation	After Inoculation	End of the cycle
5 L balloon reactor	-	5.52 ± 0.37	6.05 ± 0.11
70 L flat panel	1.31 ± 1.39	5.60 ± 0.56	6.54 ± 0.47
60 L bubble column	0.47 ± 0.66	5.37 ± 0.04	6.38 ± 0.87

3.4.4 MAINTENANCE REQUIREMENTS

In order to understand if the autotrophic scale-up process would improve with the addition of a bubble column PBR system, there was the need to compare this system with the other two on different aspects, while always obtaining a 60 L volume of each system (Table 10). The use of water and medium for cultivation was the same per liter of reactor volume in all systems.

Number of reactors:

- To obtain a 60 L volume (like the bubble column the flat panel), 12 balloon reactors are needed

Implementation area:

- 0.11 m^2 is needed for a 60 L flat panel PBR.
- 0.10 m^2 is needed for a 60 L bubble column PBR.
- 1.08 m^2 is needed for 60 L of balloon reactors.

Labor work:

- Inoculation and sampling in balloon reactors were done under sterile conditions using a flame, using a high labor work time (inoculation of 120 min for 60 L of balloons). Additionally, a preparation of this reactors was also needed before being autoclaved (60 min for 60 L of balloons).

- Flat panels needed to be installed before cultivation (30 min). Labor work and time was also needed for inoculations (20 min). Furthermore, sampling for pH analysis needed to be done often because this PBRs did not contain an automated pH regulator. After harvesting, the sparger used needed to be cleaned and the plastic needed to be discarded (20 min).
- In the bubble column, labor work and time was needed for inoculations (20 min). To start the cleaning process, hoses needed to be connected to the PBR and the peristaltic pump. This system needed to be uninstalled after cleaning (40 min).

Water use:

- The bubble column presented high use of water for the cleaning process.
- Flat panels presented high use of water when the irrigation system was used. This system also presented water use for the cleaning of the spargers, but less than the previous.
- Balloon reactors presented water use for cleaning processes.

Energy use:

- The bubble column used energy for the artificial light system and the ventilator.
- Balloon reactors used energy for artificial light and autoclave.

Waste:

- Each flat panel was made of a plastic bag which was discarded after harvesting, leading to high use of plastic (1.3 m^2 for a 60 L flat panel).
- Each balloon reactor needed aluminum foil to close its entrances completely (0.6 m^2 for 60 L of balloon reactors).

When comparing the three systems, the balloons presented a higher implementation area. Even though the implementation area of single reactors was similar, the area occupied by twelve balloons was almost 11-fold higher than a one bubble column reactor to obtain 60 L.

Labor work was over 2.5-fold higher than the bubble column or the flat panel when twelve balloon reactors were used.

Lastly, aluminum foil and plastic use is reduced when changing from balloons and flat panels, respectively, to bubble columns.

Table 10: Comparison of overall needs to maintain three different autotrophic cultivation systems

	Bubble column	Balloon reactor	Flat panel
Number of reactors (for 60 L)	1	12	1
Implementation area	0.10 m^2	1.08 m^2	0.11 m^2
Labor work time	60 min (inoculation; cleaning)	180 min (preparation; inoculation)	70 (installation; inoculation; cleaning)
Water use	High (cleaning process)	Medium (cleaning process)	High (irrigation system; cleaning of spargers)
Energy use	High (light system; ventilator)	High (light system; autoclave)	-
Waste	-	Medium (aluminum foil)	High (discharge of plastic bags)

4 CONCLUSIONS AND FUTURE PERSPECTIVES

Microalgae can be grown using different types of photobioreactors. All photobioreactors present distinct advantages and disadvantages, specially related to sterility, operation, productivity, product quality, and costs. In this work, a bubble column photobioreactor was tested and modified to reach an optimized state.

The addition of a sparger in the bubble column photobioreactor improved aeration and consequently mixing was improved. Moreover, the addition of a pH controller provided pH regulation and consequently reduced labor work. These changes provided an increase of 18 % and 5 % in maximum productivity and specific growth rate, respectively.

Three light systems were also added and compared. The installation of a light system in the back of the reactor containing 18 yellow LEDs in a metal sheet provided an overall 2.9-fold increase in maximum productivity. The other two light systems consisted of two metal sheets (one in the front and another in the back of the reactor) with 3 LEDs each, one system with white and the other with yellow lights. These systems provided an increase of 3.7-fold and 1.9-fold in maximum productivity, respectively. On the other hand, regarding the maximum specific growth rates of the light systems in the back and front of the reactor, the associated error was too high, making this parameter non credible for comparison. Hereafter, it would be interesting to do more trials under these conditions in order to reach credible conclusions. Additionally, protein and total carotenoid levels were lower in the system with 18 LEDs. Moreover, it would be interesting to do more trials under different color light systems to understand their influence on microalgal biochemical profile.

Furthermore, to understand if the bubble column photobioreactor is compatible with other species, it would be interesting to cultivate different microalgae species in the system.

Additionally, since the semi-continuous regime tested in this project was unsuccessful due high dilution rates, it would be interesting to repeat the trial (using different approaches, such as renovation based on biomass concentration or increase of the time in between renovations). It would also be interesting to install the required equipment to operate in a continuous regime.

The bubble column PBR system was also compared with other two in-house systems, a 5 L balloon reactor and a 70 L flat panel PBR system. The bubble column system presented statistically higher global and maximum areal productivity, and maximum volumetric productivity. Regarding the maximum areal productivity, values of 147.33 ± 43.99 g m^{-2} d^{-1}, 61.41 ± 12.81 g m^{-2} d^{-1}, and 6.42 ± 0.77 g m^{-2} d^{-1} were reached in bubble columns, flat panels, and balloons, respectively. In terms of biochemical profiles,

statistically higher protein content in balloons was obtained and statistically lower total carotenoid levels were presented in flat panels.

When comparing the three systems under the same volume (60 L), the balloons presented a higher implementation area. Even though the implementation area of single reactors was similar, the area occupied by twelve balloons was almost 11-fold higher than a one bubble column reactor to obtain 60 L. Labor work was over 2.5-fold higher than the bubble column or the flat panel when twelve balloon reactors were used. Lastly, aluminum foil and plastic use was reduced when changing from balloons and flat panels, respectively, to bubble columns, resulting in a reduction of overall ecological footprint. In conclusion, the scale-up autotrophic process regarding a step with a 60 L system, would be improved with the addition of a bubble column regarding occupied area, labor work, and waste. Henceforward, to reduce the high energy use by the bubble columns, this system could be installed outdoors.

REFERENCES

1. Ng, D. H. P., Ng, Y. K., Shen, H., & Lee, Y. K. (2015). Microalgal Biotechnology. In *Handbook of Marine Microalgae* (pp. 69–80). Elsevier. https://doi.org/10.1016/B978-0-12-800776-1.00006-6
2. Islam, M. A. (2014). *Microalgae: an alternative source of biodiesel for the compression ignition (CI) engine*. Science and Engineering Faculty, Queensland University of Technology.
3. Camacho, F., Macedo, A., & Malcata, F. (2019). Potential Industrial Applications and Commercialization of Microalgae in the Functional Food and Feed Industries: A Short Review. *Marine Drugs*, *17*(6), 312. https://doi.org/10.3390/md17060312
4. Queiroz, M. I., Vieira, J. G., & Maroneze, M. M. (2020). Morphophysiological, structural, and metabolic aspects of microalgae. In *Handbook of Microalgae-Based Processes and Products* (pp. 25–48). Elsevier. https://doi.org/10.1016/B978-0-12-818536-0.00002-6
5. Venkatesan, J., Manivasagan, P., & Kim, S.-K. (2015). Marine Microalgae Biotechnology. In *Handbook of Marine Microalgae* (pp. 1–9). Elsevier. https://doi.org/10.1016/B978-0-12-800776-1.00001-7
6. Giordano, M., & Wang, Q. (2018). Microalgae for Industrial Purposes. In *Biomass and Green Chemistry* (pp. 133–167). Cham: Springer International Publishing. https://doi.org/10.1007/978-3-319-66736-2_6
7. Pavlik, D., Zhong, Y., Daiek, C., Liao, W., Morgan, R., Clary, W., & Liu, Y. (2017). Microalgae cultivation for carbon dioxide sequestration and protein production using a high-efficiency photobioreactor system. *Algal Research*, *25*(April), 413–420. https://doi.org/10.1016/j.algal.2017.06.003
8. Fernández, I., Acién, F. G., Berenguel, M., & Guzmán, J. L. (2014). First Principles Model of a Tubular Photobioreactor for Microalgal Production. *Industrial & Engineering Chemistry Research*, *53*(27), 11121–11136. https://doi.org/10.1021/ie501438r
9. Huang, Q., Jiang, F., Wang, L., & Yang, C. (2017). Design of Photobioreactors for Mass Cultivation of Photosynthetic Organisms. *Engineering*, *3*(3), 318–329. https://doi.org/10.1016/J.ENG.2017.03.020
10. Mata, T. M., Martins, A. A., & Caetano, N. S. (2010). Microalgae for biodiesel production and other applications: A review. *Renewable and Sustainable Energy Reviews*, *14*(1), 217–232. https://doi.org/10.1016/j.rser.2009.07.020
11. Nwoba, E. G., Parlevliet, D. A., Laird, D. W., Alameh, K., & Moheimani, N. R. (2019). Light

management technologies for increasing algal photobioreactor efficiency. *Algal Research*, *39*(January), 101433. https://doi.org/10.1016/j.algal.2019.101433

12. Raven, J. A., & Giordano, M. (2014). Algae. *Current Biology*, *24*(13), R590–R595. https://doi.org/10.1016/j.cub.2014.05.039
13. Mobin, S., & Alam, F. (2017). Some Promising Microalgal Species for Commercial Applications: A review. *Energy Procedia*, *110*(December 2016), 510–517. https://doi.org/10.1016/j.egypro.2017.03.177
14. Ziganshina, E. E., Bulynina, S. S., & Ziganshin, A. M. (2020). Comparison of the Photoautotrophic Growth Regimens of Chlorella sorokiniana in a Photobioreactor for Enhanced Biomass Productivity. *Biology*, *9*(7), 169. https://doi.org/10.3390/biology9070169
15. Zuccaro, G., Yousuf, A., Pollio, A., & Steyer, J.-P. (2020). Microalgae Cultivation Systems. In *Microalgae Cultivation for Biofuels Production* (pp. 11–29). Elsevier. https://doi.org/10.1016/B978-0-12-817536-1.00002-3
16. Hernández-Pérez, A., & Labbé, J. I. (2014). Microalgas, cultivo y beneficios. *Revista de biología marina y oceanografía*, *49*(2), 157–173. https://doi.org/10.4067/S0718-19572014000200001
17. Park, J. B. K., Craggs, R. J., & Shilton, A. N. (2011). Wastewater treatment high rate algal ponds for biofuel production. *Bioresource Technology*, *102*(1), 35–42. https://doi.org/10.1016/j.biortech.2010.06.158
18. Singh, N. K., & Dhar, D. W. (2011). Microalgae as second generation biofuel. A review. *Agronomy for Sustainable Development*, *31*(4), 605–629. https://doi.org/10.1007/s13593-011-0018-0
19. Yi, Z., Su, Y., Cherek, P., Nelson, D. R., Lin, J., Rolfsson, O., ... Fu, W. (2019). Combined artificial high-silicate medium and LED illumination promote carotenoid accumulation in the marine diatom Phaeodactylum tricornutum. *Microbial Cell Factories*, *18*(1), 209. https://doi.org/10.1186/s12934-019-1263-1
20. Daboussi, F., Leduc, S., Maréchal, A., Dubois, G., Guyot, V., Perez-Michaut, C., ... Duchateau, P. (2014). Genome engineering empowers the diatom Phaeodactylum tricornutum for biotechnology. *Nature Communications*, *5*(1), 3831. https://doi.org/10.1038/ncomms4831
21. Yang, Z.-K., Niu, Y.-F., Ma, Y.-H., Xue, J., Zhang, M.-H., Yang, W.-D., ... Li, H.-Y. (2013). Molecular and cellular mechanisms of neutral lipid accumulation in diatom following nitrogen deprivation. *Biotechnology for Biofuels*, *6*(1), 67. https://doi.org/10.1186/1754-6834-6-67
22. Quelhas, P. M., Trovão, M., Silva, J. T., Machado, A., Santos, T., Pereira, H., ... Silva, J. L. (2019).

Industrial production of Phaeodactylum tricornutum for CO2 mitigation: biomass productivity and photosynthetic efficiency using photobioreactors of different volumes. *Journal of Applied Phycology*, *31*(4), 2187–2196. https://doi.org/10.1007/s10811-019-1750-0

23. Ovide, C., Kiefer-Meyer, M.-C., Bérard, C., Vergne, N., Lecroq, T., Plasson, C., ... Bardor, M. (2018). Comparative in depth RNA sequencing of P. tricornutum's morphotypes reveals specific features of the oval morphotype. *Scientific Reports*, *8*(1), 14340. https://doi.org/10.1038/s41598-018-32519-7
24. Fajardo, A. R., Cerdán, L. E., Medina, A. R., Fernández, F. G. A., Moreno, P. A. G., & Grima, E. M. (2007). Lipid extraction from the microalga Phaeodactylum tricornutum. *European Journal of Lipid Science and Technology*, *109*(2), 120–126. https://doi.org/10.1002/ejlt.200600216
25. Perez-Garcia, O., Escalante, F. M. E., De-Bashan, L. E., & Bashan, Y. (2011). Heterotrophic cultures of microalgae: Metabolism and potential products. *Water Research*, *45*(1), 11–36. https://doi.org/10.1016/j.watres.2010.08.037
26. Zhan, J., Rong, J., & Wang, Q. (2017). Mixotrophic cultivation, a preferable microalgae cultivation mode for biomass/bioenergy production, and bioremediation, advances and prospect. *International Journal of Hydrogen Energy*, *42*(12), 8505–8517. https://doi.org/10.1016/j.ijhydene.2016.12.021
27. Chojnacka, K., & . F.-J. M. (2003). Kinetic and Stoichiometric Relationships of the Energy and Carbon Metabolism in the Culture of Microalgae. *Biotechnology(Faisalabad)*, *3*(1), 21–34. https://doi.org/10.3923/biotech.2004.21.34
28. Fernández, F. G. A., Fernández-Sevilla, J. M., Moya, B. L., & Grima, E. M. (2020). Microalgae production systems. In *Handbook of Microalgae-Based Processes and Products* (pp. 127–163). Elsevier. https://doi.org/10.1016/B978-0-12-818536-0.00006-3
29. Ounnar, A., Kaidi, F., Benhabyles, L., & Aziza, M. A. (2015). Investigation of Photobioreactor Design for Biomass Production by Green Microalgae. In I. Dincer, C. O. Colpan, O. Kizilkan, & M. A. Ezan (Eds.), *Progress in Clean Energy, Volume 2* (Vol. 2, pp. 83–92). Cham: Springer International Publishing. https://doi.org/10.1007/978-3-319-17031-2_7
30. Merchuk, J. C. (2020). Photobioreactor design. In *Handbook of Microalgae-Based Processes and Products* (pp. 101–126). Elsevier. https://doi.org/10.1016/B978-0-12-818536-0.00005-1
31. Koller, M. (2015). Design of Closed Photobioreactors for Algal Cultivation. In *Algal Biorefineries* (pp. 133–186). Cham: Springer International Publishing. https://doi.org/10.1007/978-3-319-20200-6_4

32. Hallmann, A. (2016). Algae Biotechnology – Green Cell-Factories on the Rise. *Current Biotechnology*, *4*(4), 389–415. https://doi.org/10.2174/2211550105666151107001338

33. Krishnan, A., Likhogrud, M., Cano, M., Edmundson, S., Melanson, J. B., Huesemann, M., … Posewitz, M. C. (2021). Picochlorum celeri as a model system for robust outdoor algal growth in seawater. *Scientific Reports*, *11*(1), 11649. https://doi.org/10.1038/s41598-021-91106-5

34. Cunha, P. (2019). *Optimization of Nannochloropsis oceanica cultivation in pilot-scale raceway ponds*. Faculty of Engineering, University of Porto.

35. Pulz, O. (2001). Photobioreactors: production systems for phototrophic microorganisms. *Applied Microbiology and Biotechnology*, *57*(3), 287–293. https://doi.org/10.1007/s002530100702

36. Chew, K. W., Chia, S. R., Show, P. L., Yap, Y. J., Ling, T. C., & Chang, J.-S. (2018). Effects of water culture medium, cultivation systems and growth modes for microalgae cultivation: A review. *Journal of the Taiwan Institute of Chemical Engineers*, *91*, 332–344. https://doi.org/10.1016/j.jtice.2018.05.039

37. Ting, H., Haifeng, L., Shanshan, M., Zhang, Y., Zhidan, L., & Na, D. (2017). Progress in microalgae cultivation photobioreactors and applications in wastewater treatment: A review. *International Journal of Agricultural and Biological Engineering*, *10*(1), 1–29. https://doi.org/10.3965/j.ijabe.20171001.2705

38. Van Stappen, G. (1996). Introduction, biology and ecology of Artemia. In P. Lavens & P. Sorgeloos (Eds.), *Manual on the production and use of live food for aquaculture* (pp. 79–106). Rome, Italy: FAO. Retrieved from https://biblio.ugent.be/publication/4245243

39. Zohri, A. A., Ragab, S. W., Mekawi, M. I., & Mostafa, O. A. A. (2017). Comparison Between Batch, Fed-Batch, Semi-Continuous and Continuous Techniques for Bio-Ethanol Production from a Mixture of Egyptian Cane and Beet Molasses. *Egyptian Sugar Journal*, *9*, 89–111. Retrieved from https://www.researchgate.net/publication/319318923

40. Brown, M. R., Garland, C. D., Jeffrey, S. W., Jameson, I. D., & Leroi, J. M. (1993). The gross and amino acid compositions of batch and semi-continuous cultures of Isochrysis sp. (clone T.ISO), Pavlova lutheri and Nannochloropsis oculata. *Journal of Applied Phycology*, *5*(3), 285–296. https://doi.org/10.1007/BF02186231

41. Bharguram, L. S. (1999). *High Density Culture of Marine Microalgae Using Semi-Continuous and Continuous Systems*. Central Institute of Fisheries Education. Retrieved from http://eprints.cmfri.org.in/11077/

42. Guerra, I. F. (2019). *Comparison of microalgae grown at pilot-scale under different operation*

regimes. Instituto Superior Técnico, Universidade de Lisboa.

43. Cultivando Soluções Sustentáveis de Microalgas – Allmicralgae. (n.d.). Retrieved November 2, 2021, from https://www.allmicroalgae.com/pt-pt/
44. Notícias. (n.d.). Retrieved November 2, 2021, from https://www.compete2020.gov.pt/noticias/detalhe/Proj17608-FermALG-SecII-IDT-NL156-24052018
45. ALLMICROALGAE - AlgaValor. (n.d.). Retrieved November 2, 2021, from https://www.algavalor.pt/en/customer/allmicroalgae/
46. Ruiz, J., Álvarez-Díaz, P. D., Arbib, Z., Garrido-Pérez, C., Barragán, J., & Perales, J. A. (2013). Performance of a flat panel reactor in the continuous culture of microalgae in urban wastewater: Prediction from a batch experiment. *Bioresource Technology*, *127*, 456–463. https://doi.org/10.1016/j.biortech.2012.09.103
47. Mata, T. M., Melo, A. C., Simões, M., & Caetano, N. S. (2012). Parametric study of a brewery effluent treatment by microalgae Scenedesmus obliquus. *Bioresource Technology*, *107*, 151–158. https://doi.org/10.1016/j.biortech.2011.12.109
48. Quelhas, P. M. (2017). *Photosynthetic efficiency and CO2 mitigation by Phaeodactylum tricornutum in industrial reactors*. Faculty of Engineering, University of Porto.
49. Barros, A., Pereira, H., Campos, J., Marques, A., Varela, J., & Silva, J. (2019). Heterotrophy as a tool to overcome the long and costly autotrophic scale-up process for large scale production of microalgae. *Scientific Reports*, *9*(1), 13935. https://doi.org/10.1038/s41598-019-50206-z
50. Conde, T. A., Neves, B. F., Couto, D., Melo, T., Neves, B., Costa, M., … Domingues, M. R. (2021). Microalgae as sustainable bio-factories of healthy lipids: Evaluating fatty acid content and antioxidant activity. *Marine Drugs*, *19*(7), 1–20. https://doi.org/10.3390/md19070357
51. Meteorologia mensal em Pataias, Leiria, Portugal | AccuWeather. (n.d.). Retrieved from https://www.accuweather.com/pt/pt/pataias/861200/september-weather/861200?year=2021
52. Reddy, K. R., Sabyasachi, S., Meshram, P. M., & Borghate, V. B. (2016). An asymmetrical multilevel inverter topology with reduced source count. In *2016 IEEE Students' Conference on Electrical, Electronics and Computer Science (SCEECS)* (Vol. 41, pp. 1–6). IEEE. https://doi.org/10.1109/SCEECS.2016.7509296
53. The Algem photobioreactor | Algenuity. (n.d.). Retrieved from https://www.algenuity.com/algem
54. Fernández, F. G. A., Pérez, J. A. S., Sevilla, J. M. F., Camacho, F. G., & Grima, E. M. (2000).

Modeling of eicosapentaenoic acid (EPA) production from Phaeodactylum tricornutum cultures in tubular photobioreactors. Effects of dilution rate, tube diameter, and solar irradiance. *Biotechnology and Bioengineering*, *68*(2), 173–183. https://doi.org/10.1002/(SICI)1097-0290(20000420)68:2<173::AID-BIT6>3.0.CO;2-C

55. Branco-Vieira, M., San Martin, S., Agurto, C., Santos, M., Freitas, M., Mata, T., … Caetano, N. (2017). Potential of Phaeodactylum tricornutum for Biodiesel Production under Natural Conditions in Chile. *Energies*, *11*(1), 54. https://doi.org/10.3390/en11010054
56. Climate Change and Harmful Algal Blooms | US EPA. (n.d.). Retrieved from https://www.epa.gov/nutrientpollution/climate-change-and-harmful-algal-blooms
57. Nur, M. M. A., Muizelaar, W., Boelen, P., & Buma, A. G. J. (2019). Environmental and nutrient conditions influence fucoxanthin productivity of the marine diatom Phaeodactylum tricornutum grown on palm oil mill effluent. *Journal of Applied Phycology*, *31*(1), 111–122. https://doi.org/10.1007/s10811-018-1563-6
58. Di Lena, G., Casini, I., Lucarini, M., & Lombardi-Boccia, G. (2019). Carotenoid profiling of five microalgae species from large-scale production. *Food Research International*, *120*, 810–818. https://doi.org/10.1016/j.foodres.2018.11.043
59. Guerra, I., Pereira, H., Costa, M., Silva, J. T., Santos, T., Varela, J., … Silva, J. (2021). Operation Regimes: A Comparison Based on Nannochloropsis oceanica Biomass and Lipid Productivity. *Energies*, *14*(6), 1542. https://doi.org/10.3390/en14061542
60. Maia, I. B., Carneiro, M., Magina, T., Malcata, F. X., Otero, A., Navalho, J., … Pereira, H. (2022). Diel biochemical and photosynthetic monitorization of Skeletonema costatum and Phaeodactylum tricornutum grown in outdoor pilot-scale flat panel photobioreactors. *Journal of Biotechnology*, *343*(August 2021), 110–119. https://doi.org/10.1016/j.jbiotec.2021.11.008

APPENDIX A

CALIBRATION CURVE

The calibration curve for *Phaeodactylum tricornutum* (strain 0079PN) was obtained using experimental points from which was measured the optical density and DW of the same sample.

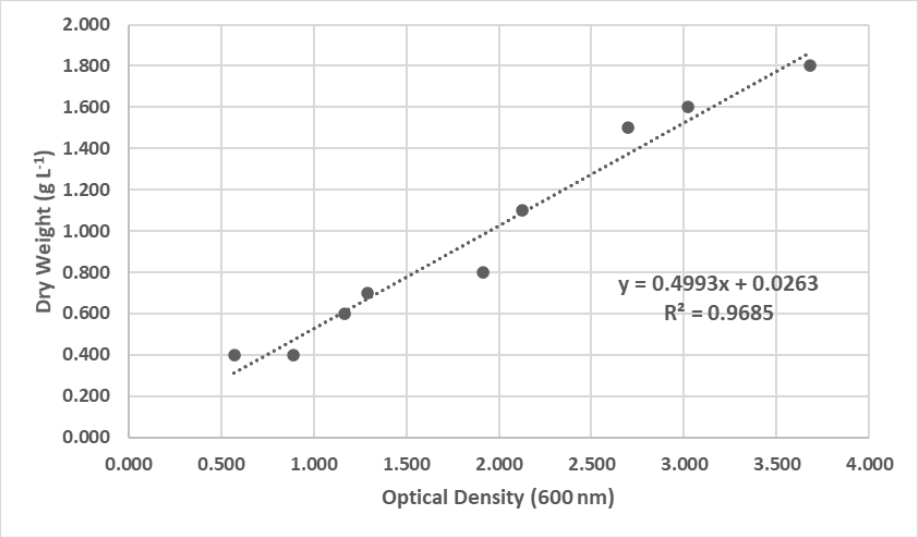

Figure 39: Correlation between the optical density at 600 nm and the DW of an autotrophic culture of *Phaeodactylum tricornutum* (strain 0079PN).

APPENDIX B

GROWTH CURVES

Growth curves for the trials done in Chapter 3.3.1 and Chapter 3.3.2.

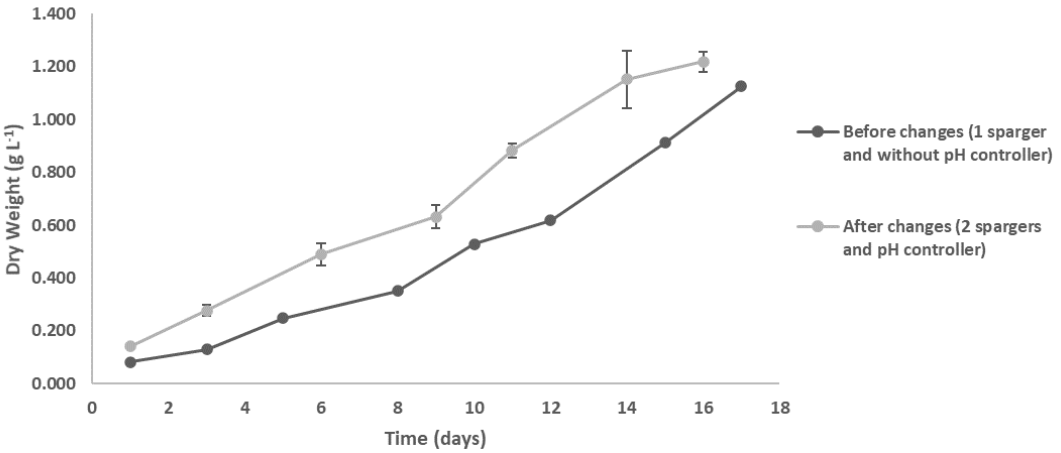

Figure 40: Growth curve of *Phaeodactylum tricornutum*, cultivated in 60 L bubble column photobioreactors. The values of the line after changes presented are the average values of the two independent biological replicates and the error bars are the respective standard deviations.

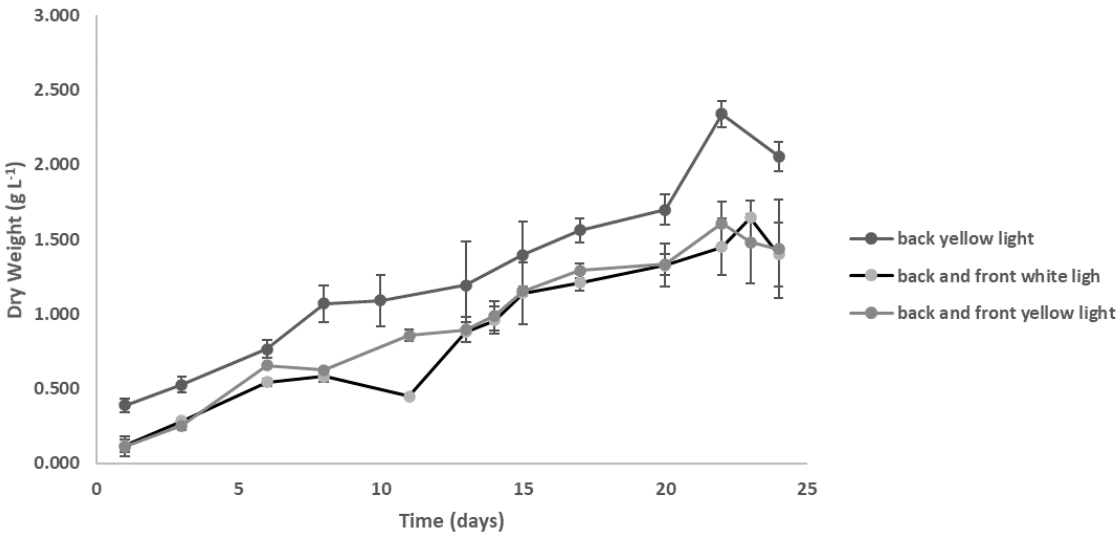

Figure 41: Growth curve of *Phaeodactylum tricornutum*, cultivated in 60 L bubble column photobioreactors. The values presented are the average values of the two independent biological replicates and the error bars are the respective standard deviations.

APPENDIX C

PHOTON FLUX DENSITY

The photon flux density (µmol m^{-2} s^{-1}) of the light was measured at different distances of the lights to the reactor. The results for the remaining distances, in each stage (36 stages – as 36th being the maximum intensity reached by the system - divided in four: 9, 18, 27, and 36) and each point on the reactor (being point 1 and 3 shown as a single point on the side of the reactor and point 2 as the front) are shown in Figure 42, Figure 43, Figure 44, and Figure 45.

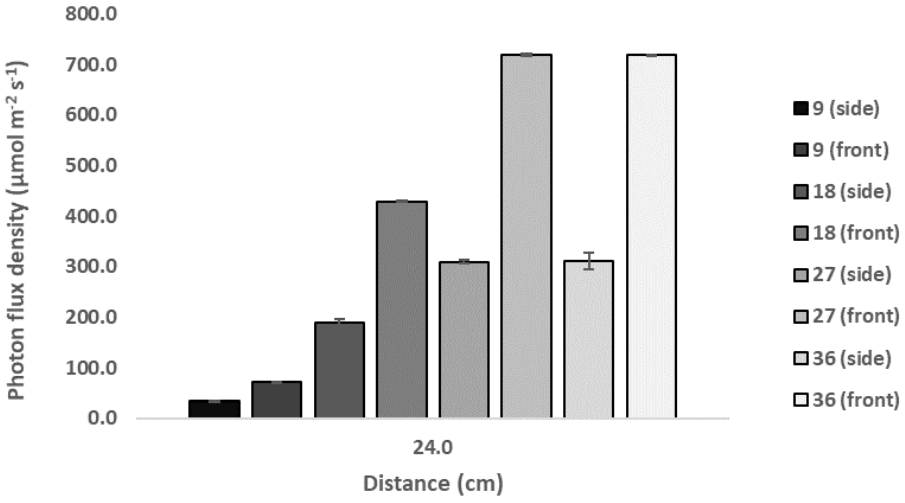

Figure 42: Photon flux density in different stages of light intensity and in two different points of the bubble column photobioreactor, front and side, at a 24.0 cm distance. The values presented are the average values of the three independent replicates and the error bars are the respective standard deviations.

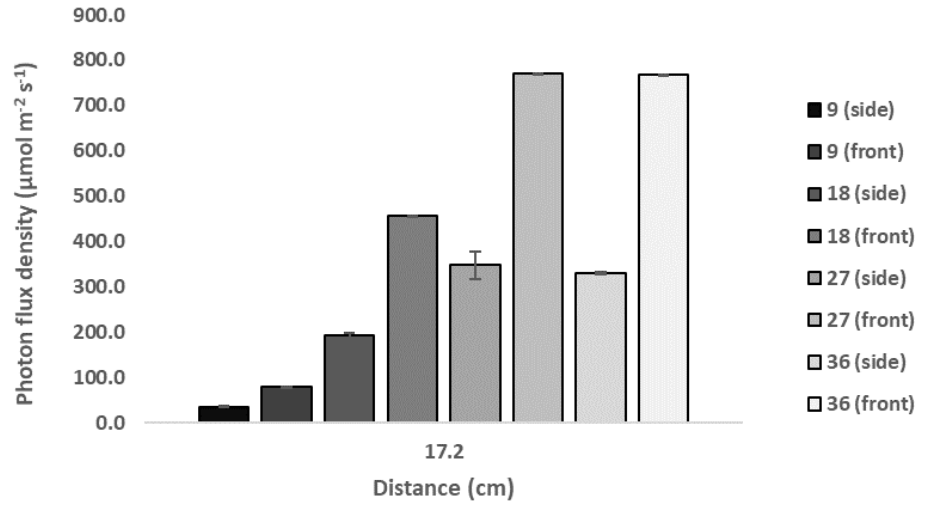

Figure 43: Photon flux density in different stages of light intensity and in two different points of the bubble column photobioreactor, front and side, at a 17.2 cm distance. The values presented are the average values of the three independent replicates and the error bars are the respective standard deviations.

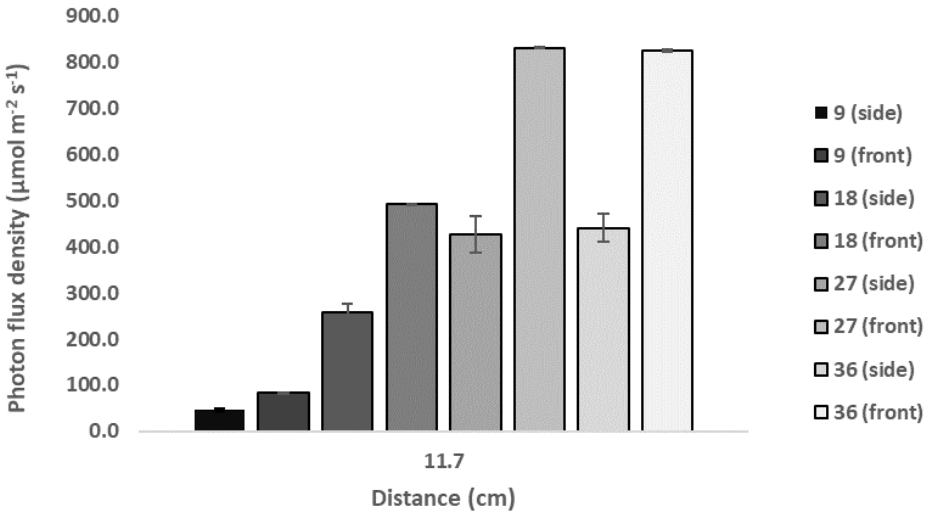

Figure 44: Photon flux density in different stages of light intensity and in two different points of the bubble column photobioreactor, front and side, at a 11.7 cm distance. The values presented are the average values of the three independent replicates and the error bars are the respective standard deviations.

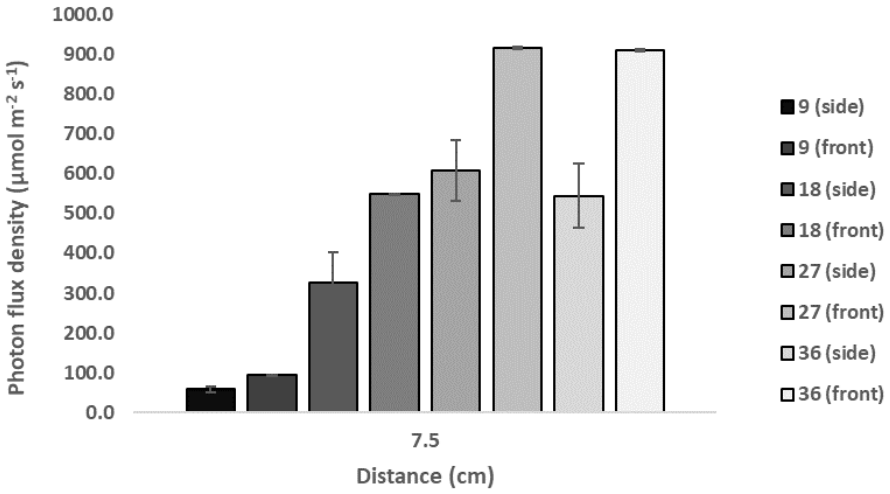

Figure 45: Photon flux density in different stages of light intensity and in two different points of the bubble column photobioreactor, front and side, at a 7.5 cm distance. The values presented are the average values of the three independent replicates and the error bars are the respective standard deviations.